(2)

AR-006-326

# *Analytical Calculations of Fatigue Loading of Submarine Hulls*

*I.M. Robertson*

MRL Technical Report
MRL-TR-90-26

## *Abstract*

*Fatigue is a potential failure mode of submarine pressure hulls. Australia's new Type 471 submarines will be constructed from a new high strength steel. The higher design loadings made possible by the higher strength make fatigue an even more significant consideration than in other designs. The stress analysis of submarine pressure hulls under hydrostatic loading is reviewed. The main emphasis is on analytical methods of calculation as opposed to numerical (e.g. finite element) methods, and on the calculation of the fatigue loading rather than the calculation of buckling pressure. Because of the emphasis on fatigue, stress concentrations, residual stresses and the interaction between residual and applied stresses are considered.*



MATERIALS RESEARCH LABORATORY

*Published by*

*DSTO Materials Research Laboratory*
*Cordite Avenue, Maribyrnong*
*Victoria 3032, Australia*

*Telephone: (03) 319 3887*
*Fax: (03) 318 4536*


*AR No. 006-326*

# *Author*

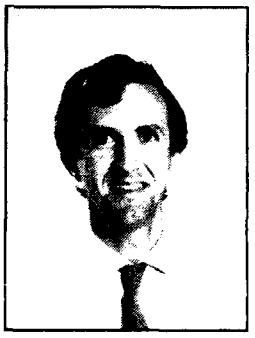

## *Ian Robertson*

*Dr Ian Robertson graduated BMet (Hons) from the University of Newcastle in 1979, and was awarded a PhD in Metallurgical Engineering from the University of Illinois in 1983. He joined MRL in 1988, where his main interests have been magnetic properties of ferromagnetic materials, and fatigue of welded structures. He has broad experience in ferrous and non-ferrous metallurgy, and modern techniques for materials characterization.*

# *Contents*

# *Analytical Calculation of Fatigue Loading of Submarine Hulls*

## *1. Introduction*

The following introductory remarks are based on reviews of the subject by Wenk (1961), Kendrick (1985) and Bushnell (1985). Submarine pressure hulls are the world's largest pressure vessels. The major design loading is the external hydrostatic pressure at depth, but a submarine hull is also subject to hydrodynamic stresses, and possibly to stresses arising from enemy attack. The stress analysis of the hulls is a well-developed science because it is important to produce a hull of minimum weight in order to retain sufficient buoyancy for propulsion systems, weapons and sensors. Accurate stress analysis results in precision design and the confident use of safety factors of the order of 1.5 or less. Accuracy in strength prediction has been confirmed by tests to destruction of small and large scale models, and by strain gauging of submarines.

A submarine pressure hull typically consists of a cylindrical centre section closed at the ends with spherical or torispherical caps. Some examples are shown in Figure 1. The caps are usually convex, but may be concave (as viewed from outside the submarine) or even flat as in many Kockums designs. The cross section may be tapered towards the ends by the insertion of conical sections. More general shapes are also possible, including figure-of-eight or even triple-hulled cross sections, or more fish-shaped single hull configurations. A recent Italian design consists of numerous toroids welded together (Compton-Hall, 1989).

The challenge for stress analysts is to calculate the extent of stress concentration at transitions (e.g. between the end caps and remainder of the hull, cone-cylinder transitions), at hull penetrations, and at other structural discontinuities such as bulkhead locations.

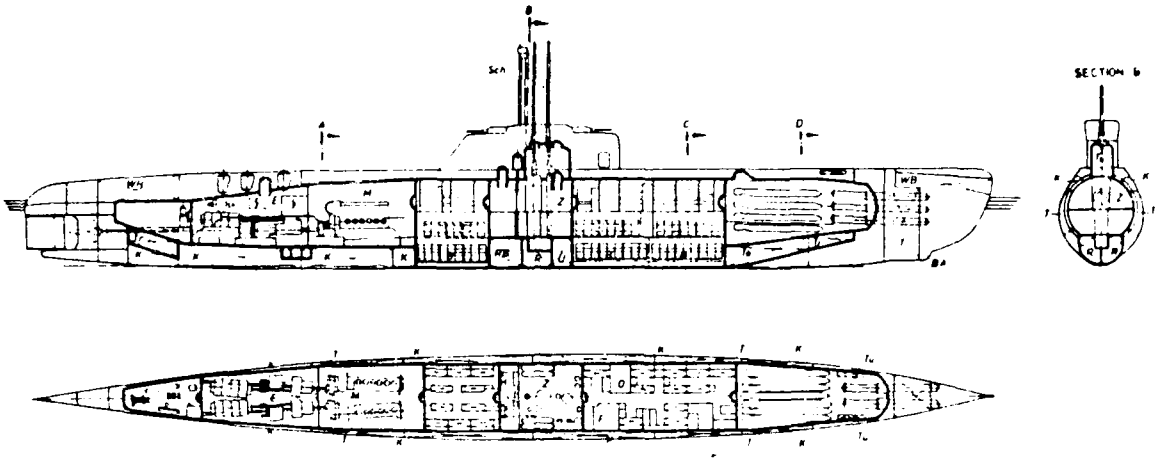

*(a) German Type XXI U-boat*

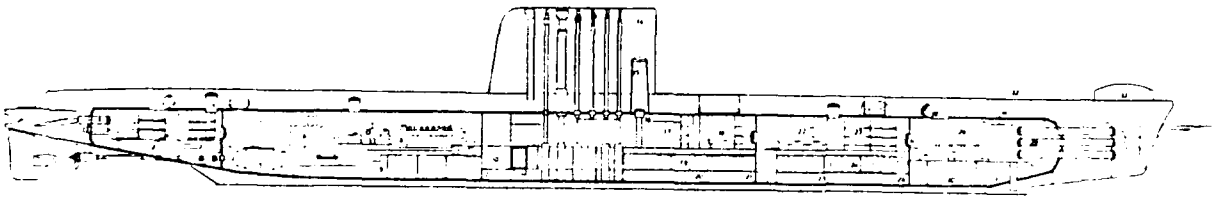

*(b) British Oberon class*

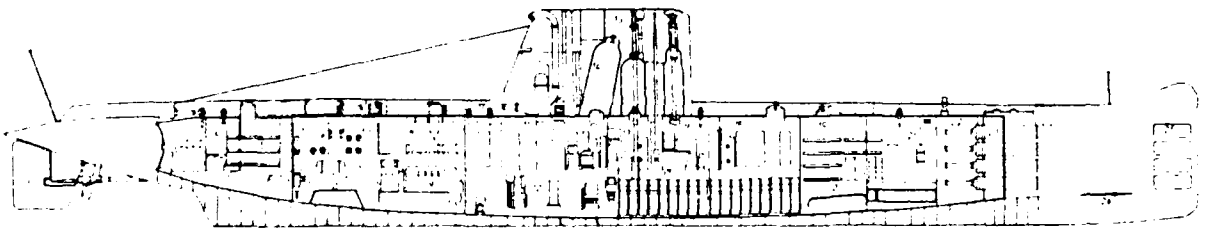

*(c) French Daphne class*

*Figure 1: Examples of SSK submarine hull designs (from Friedman, 1984; Janes, 1989)*

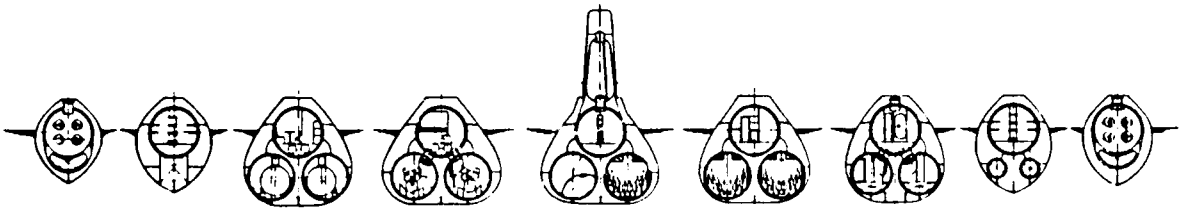

*(d) Cross-sections of Dutch Dolfijn class*

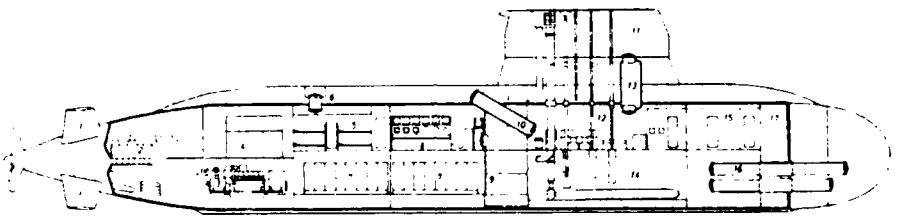

*(e) Swedish Sjoormen class (Kockums design)*

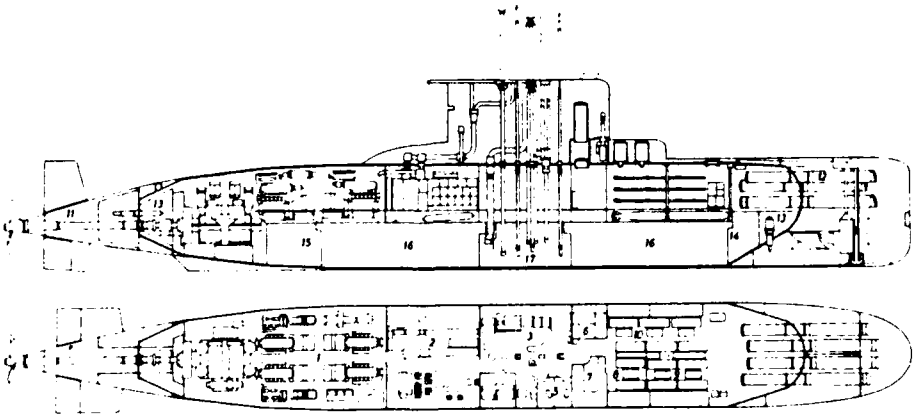

*(f) German Type 209*

*Figure 1 (continued)*

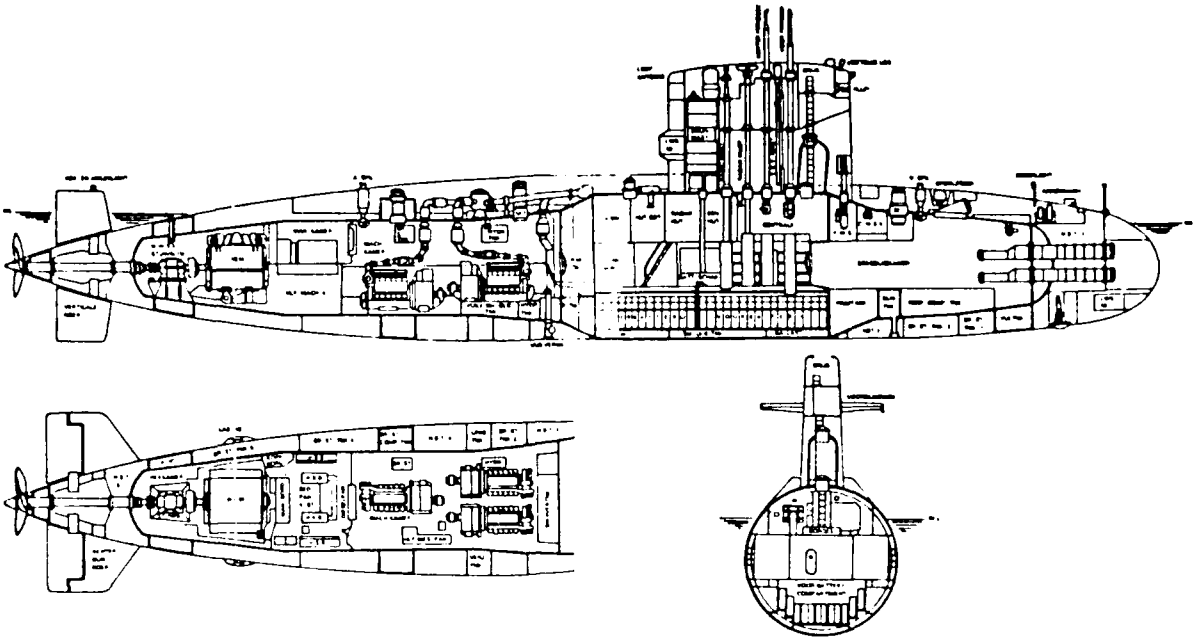

*(g) Dutch Zwaardvis class*

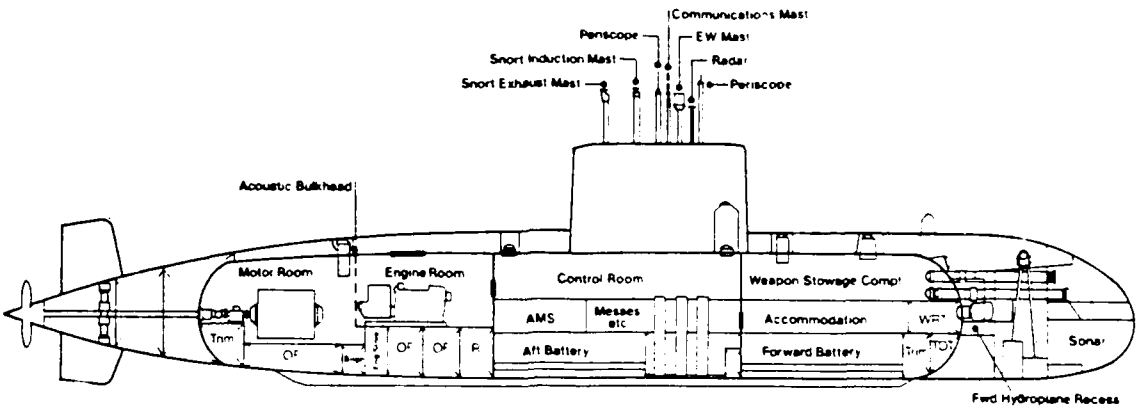


*(h) British Type 2400*

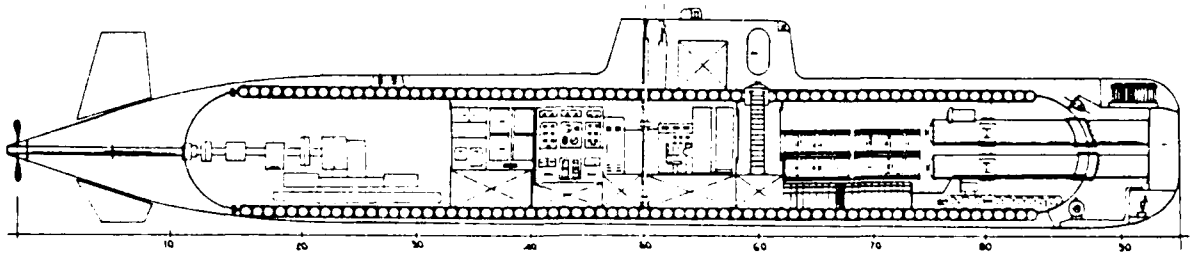

*(i) Italian 3GST9 midget submarine*

*Figure 1 (continued)*

## 2. Current Relevance

This review is concerned with the stress analysis of Australia's new Type 471 submarines for the purpose of assessing susceptibility to fatigue and corrosion fatigue. The pressure hull of the Type 471 is being constructed from a new, high strength, quenched-and-tempered steel. The susceptibility of steels to corrosion fatigue generally increases as their strength increases, only partly because the higher strength allows design for higher stresses (de Hart, 1969; Thomson and Christopher, 1973). In addition, a submarine can expect a fatigue loading of the order of $10^4$ cycles during its lifetime due to diving to depth. This puts it in the regime of low cycle or medium cycle fatigue, where increased yield strength may decrease the S-N fatigue life (Stout and Pense, 1965). Therefore the Type 471 is potentially much more susceptible to fatigue and corrosion fatigue than the Oberon.

In this context, stress analysis is not required for calculation of collapse depth or buckling mode. With the Type 471 design already established, the requirement is for calculation of stresses in the hull as a function of depth down to about two thirds of collapse depth (assuming a safety factor of 1.5). Within this range an elastic stress analysis is sufficient to obtain the necessary data for fatigue and corrosion fatigue analysis. The combination of the expected mission profile and service life of the Type 471 submarine together with the elastic stress analysis, allows a fatigue loading spectrum to be predicted.

In this report the emphasis is on analytical solutions involving hand or simple computer calculations. This provides a qualitative picture of the overall behaviour and provides calibration points for more sophisticated computer stress analysis. Axisymmetric stress analysis has become a routine process using codes such as ASSSAI and BOSOR4 (Roberts and Smith, 1988).

## 3. Simple Structures

In this section some simple structures, idealisations of a submarine hull, are examined. In subsequent sections more realistic configurations are considered. Consider first an infinitely long, circular tube subjected to uniform external pressure. The circumferential (hoop) stress is (Young, 1989):

$$\sigma_\theta = - pR / h \qquad (1)$$

and the reduction in radius is:

$$\Delta R = pR^2 / Eh \qquad (2)$$

where p is the pressure, R the radius and h the wall thickness of the cylinder.

A finite-length cylinder experiences similar hoop stress but is also subject to a longitudinal stress of:

$$\sigma_z = \sigma_\theta / 2 = - pR / 2h \qquad (3)$$

due to pressure on the end closures. The basic stress state of a submarine hull is therefore one of biaxial compression with the longitudinal stress half that in the circumferential direction. Stress concentrations in a real hull can modify this significantly in local regions and even result in regions of tensile stress.

The reduction in radius for the finite length cylinder is:

$$\Delta R = pR^2 (1 - \nu/2) / Eh \qquad (4)$$

Minimum-weight-design of a hull necessitates the use of a stiffened cylinder rather than a simple shell. Because of the large circumferential stress component, the stiffeners are in the form of circumferential rings welded to either the inside or the outside of the hull plating. The stiffening rings (or "frames") usually have a T cross section. Under pressure the shell tends to bend inward between the stiffeners forming a concertina shape. Bending stresses are introduced, and the stresses are no longer uniform through the thickness of the plating as they are in the case of a simple tube. The schematic geometry is shown in Figure 2.

## *4. Yielding, Buckling and Submarine Design*

Failure of a pressure hull at great depth may be due to yielding of the hull steel, or due to some form of buckling. The design determines which mode of failure actually takes place. The four primary modes of failure to be considered (Wenk, 1961; Kendrick, 1985) are:

(i) Yielding of the shell between the rings, characterised by an axi-symmetric concertina-shaped pleat. This is also the elastic deformation mode prior to collapse. Yielding and other failure modes are illustrated in Figure 3.

(ii) Inter-stiffener buckling ("local instability", "shell buckling") in which lobes develop between the rings. The rings are at nodes of the buckling mode, and there is usually a large number of lobes.

(iii) Stiffener tripping ("local stiffener instability") in which a ring fails by buckling.

(iv) General instability ("overall collapse") in which rings and shell fail simultaneously from one end of the stiffened cylinder to the other, with two to five circumferential lobes. In practice, general instability is probably precipitated by initial yielding or stiffener tripping.

*Figure 2: Schematic diagram showing deflection of a ring-stiffened cylinder under hydrostatic pressure to form a concertina shape.*

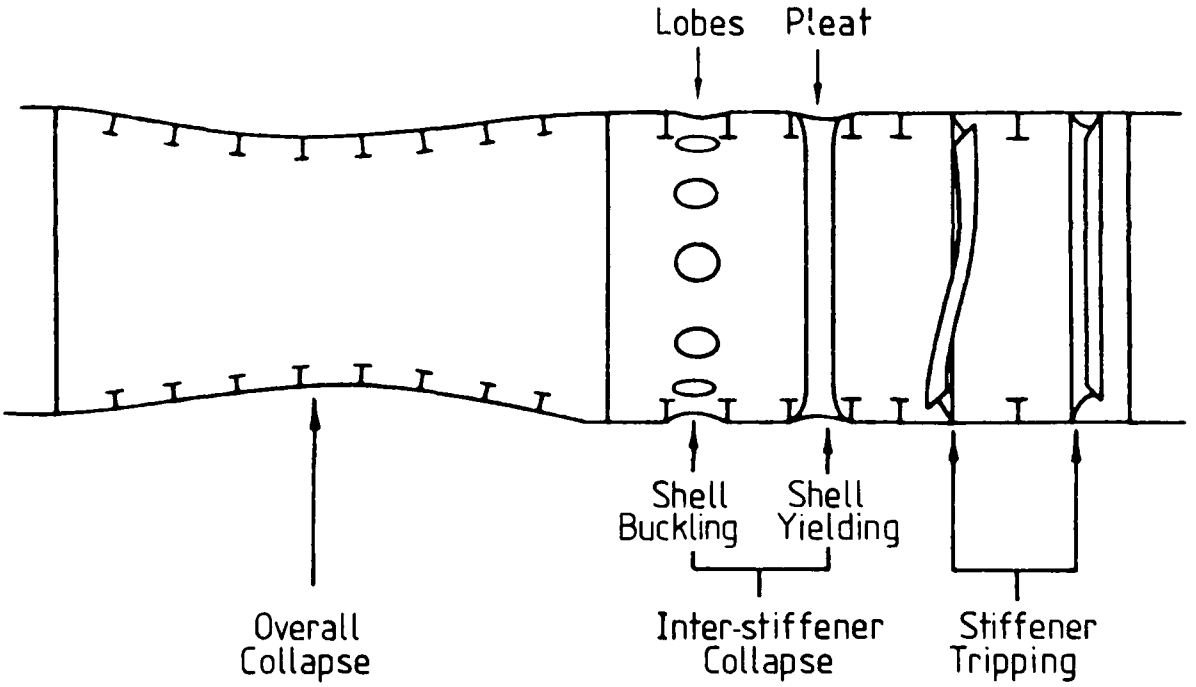


*Figure 3: Modes of collapse of a ring-stiffened cylinder (from Roberts and Smith, 1988).*

Pressure hull failure modes mirror the failure modes of a column under compression loading. Short, thick columns fail by yielding, as do hulls with thick shells and closely spaced stiffeners. Slender columns and thin shells with widely spaced stiffeners fail by buckling. The dimensions of the stiffeners determine whether shell buckling is local (heavy

stiffeners) or overall (light stiffeners), or whether tripping occurs (very light stiffeners or those with thin webs).

To illustrate the general principles of buckling, consider a simple column. A slender column under axial compression remains straight up to a critical load, $P_{cr}$, where buckling may occur. Below $P_{cr}$ the column is in stable equilibrium. Above $P_{cr}$ two equilibrium positions are possible (one straight, the other buckled). Even a small perturbation can cause the transition from straight to buckled configuration. This is known as bifurcation buckling.

For a pin-ended column the critical buckling load is (Popov, 1978):

$$P_{cr} = \pi^2 E I_x / L^2 \tag{5}$$

where E is Young's modulus, $I_x$ is the moment of inertia and L the length of the column. The corresponding critical compressive stress in the column is:

$$\sigma_{cr} = P_{cr} / A = \pi^2 E / \lambda^2 \tag{6}$$

where A is cross section and $\lambda$ the slenderness ratio, $\sqrt{I_x / L^2 A}$.

Above the critical load or stress, the buckled mode

$$w = w_o \sin (\pi z / L) \tag{7}$$

becomes possible in addition to the straight column (axisymmetric) mode w = 0, where w is the sideways deflection and z the coordinate in the axial direction.

If $\sigma_{cr}$ exceeds the yield stress of the material, $\sigma_y$, then yielding occurs rather than buckling. As yielding occurs and work hardening begins, the effective stiffness is the tangent modulus $E_t$ rather than the elastic modulus E. Therefore bifurcation buckling may occur at the point of yielding or after some plastic deformation. These ideas are summarised in Figure 4 (from Wenk, 1961). Parameters analogous to $\sigma_{cr}$ and $\lambda$ for stiffened cylindrical shells are identified and test results compared with equations analogous to equation (6).

True bifurcation buckling occurs only in unrealistic, ideal situations where the buckling deformation mode is orthogonal to the elastic deflection mode (i.e. buckling mode amplitude equals zero regardless of the extent of elastic deflection; Bushnell, 1985). In practice, geometrical imperfections and/or loading eccentricity are present, so that the buckling mode develops continuously from the initial irregularities as load is increased. Non-linear, elastic-plastic collapse (under rising load) or geometrical "snap-through" (under falling load) are the only buckling modes observed. Increasing eccentricity or initial imperfection amplitude decreases the buckling load as shown in Figure 5.

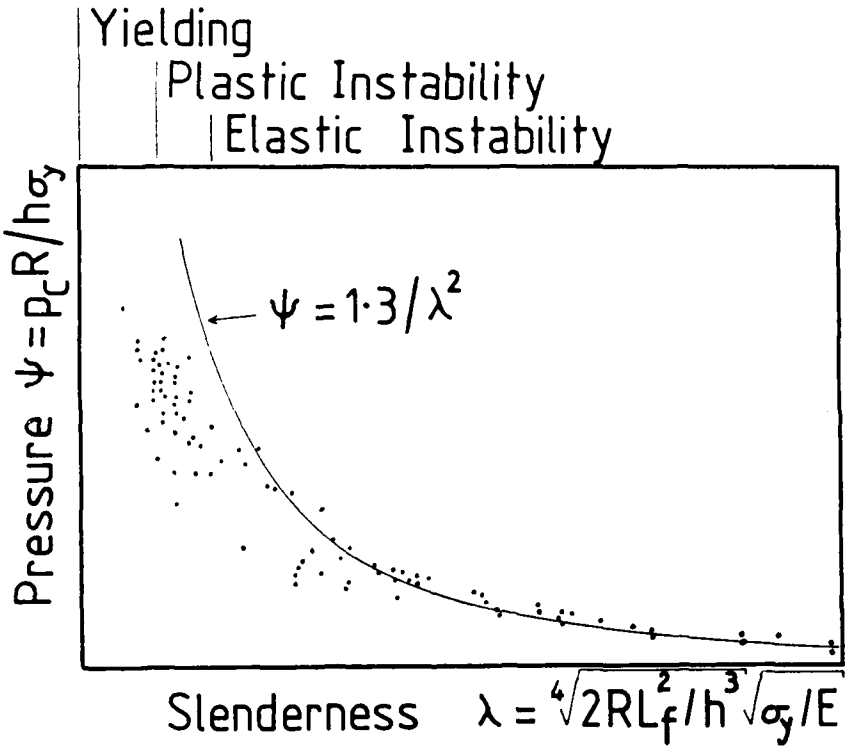


*Figure 4: Experimental data points showing the effect of slenderness ratio $\lambda$ on the failure mode and collapse pressure $p_c$ for ring-stiffened cylinders. Elastic buckling occurs for $\lambda > 1.2$ (from Wenk, 1961).*

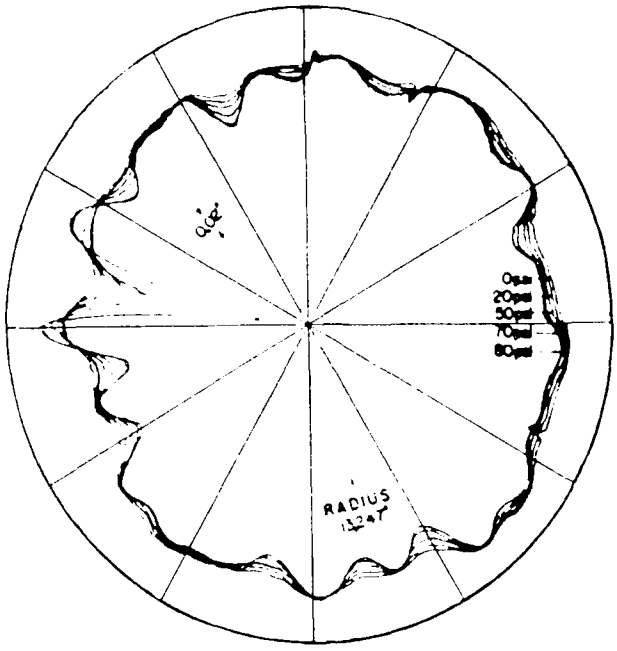


*(a) Radial deflection of an imperfect cylinder on increasing pressure from 0 to 80 psi.*

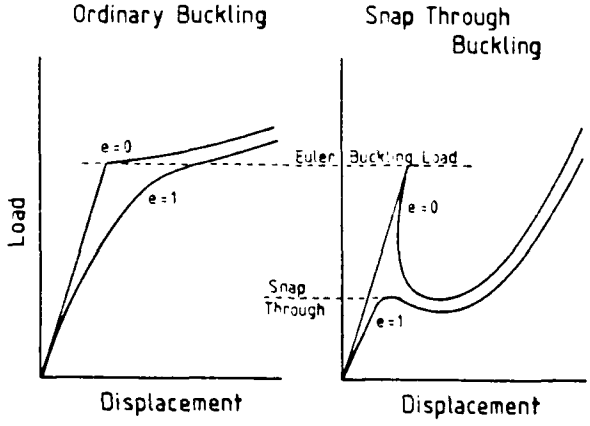


*(b) Schematic load-displacement curves for ordinary buckling (column) and snap through (spherical shell).*

*Figure 5: Effect of geometrical imperfections (or eccentricity e) on the buckling of a cylinder, column and sphere (from Wenk, 1961).*

The calculation of the critical pressure (or collapse depth) is a primary concern during the design of a submarine hull. The usual approach is to consider each possible failure mode separately. It is possible to predict $p_{cr}$ more accurately for some modes than for others, so different safety factors are applied for the different modes (for example, overall collapse is more sensitive to imperfections than other modes). The usual procedure (Kendrick, 1985) is to proportion the shell plating thickness and stiffener dimensions so that collapse at pressures in excess of the design pressure would occur by inter-stiffener collapse (with a safety factor of 1.5). Premature failure by overall collapse or local stiffener instability are avoided by applying safety factors of 2 and 4 respectively. Part of the reason for applying different safety factors is to avoid interaction between different failure modes.

In this report buckling is not a major concern. Rather the interest is in stress analysis at external pressures encountered in normal service, well below the critical buckling pressure. However, considerations of buckling largely determine the submarine design, and therefore indirectly affect the stresses and fatigue loading encountered in normal service.

# 5. *Elastic Stress Analysis of Submarine Hulls*

## *5.1 Introduction*

Much of the literature on the stress analysis of ring-stiffened cylinders, and other idealisations of submarine pressure hulls, is concerned with the prediction of buckling pressure. The calculation of elastic stresses in the hull is a much simpler task.

The early work was carried out by von Sanden and Gunther (1920) and von Mises (1929) in Germany at the time of World War I. This was extended after the war by various researchers at the David Taylor Model Basin, as reviewed by Wenk (1961). More recent reviews are those of Kendrick (1970, 1985) and Bushnell (1985).

Work prior to about 1955 emphasises analytical solution procedures and is restricted to fairly simple (but not trivial) geometries. A wide variety of general and more specific computer programs is now available for the stress analysis of structures including pressure vessels. The codes dealing with axisymmetric structures are most applicable to the stress analysis of submarine hulls.

## *5.2 Illustrative Example*

In order to gain a qualitative picture of hull stresses, consider the "typical" structure shown in Figure 6. The stress distributions at various locations obtained using NCRE's PEGASUS computer code (Kendrick, 1964) are shown in Figure 7. Away from stress concentrations other than uniformly spaced stiffeners, the general features of the stress distribution in the cylindrical sections are:

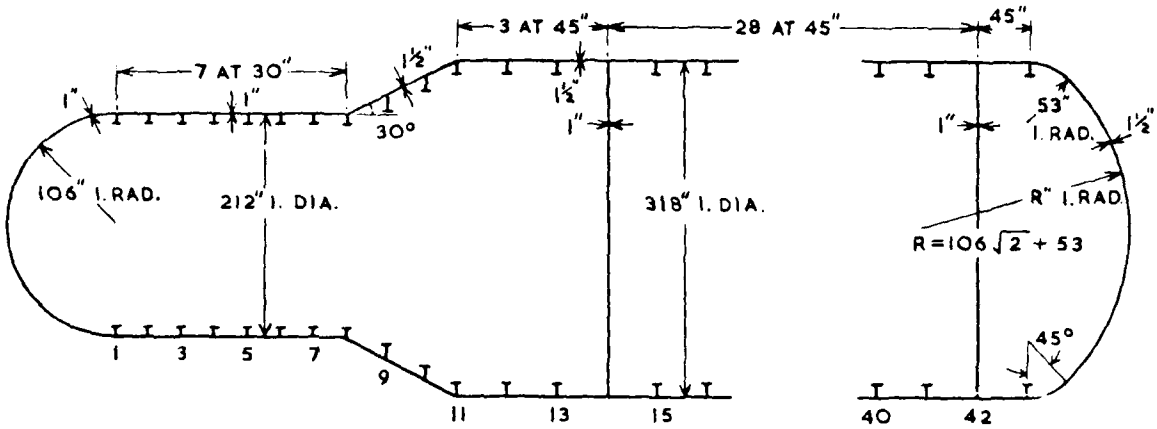


*Figure 6: Example of a typical submarine pressure hull (Kendrick, 1964).*

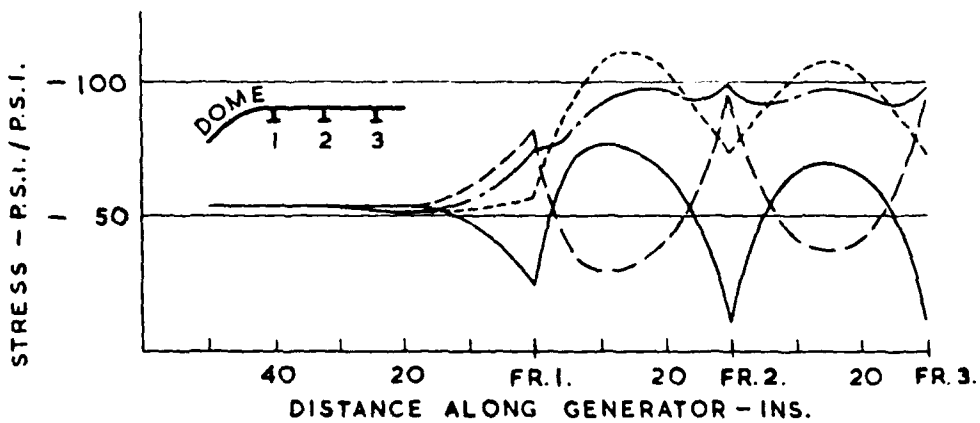


*(a) Stresses near dome-cylinder junction*

*Figure 7: Stresses in the hull plating for the structure shown in Figure 6.*

*Longitudinal* ——— *Outer surface*
— — — *Inner surface*

*Circumferential* - - - - *Outer surface*
— · — · — *Inner surface*

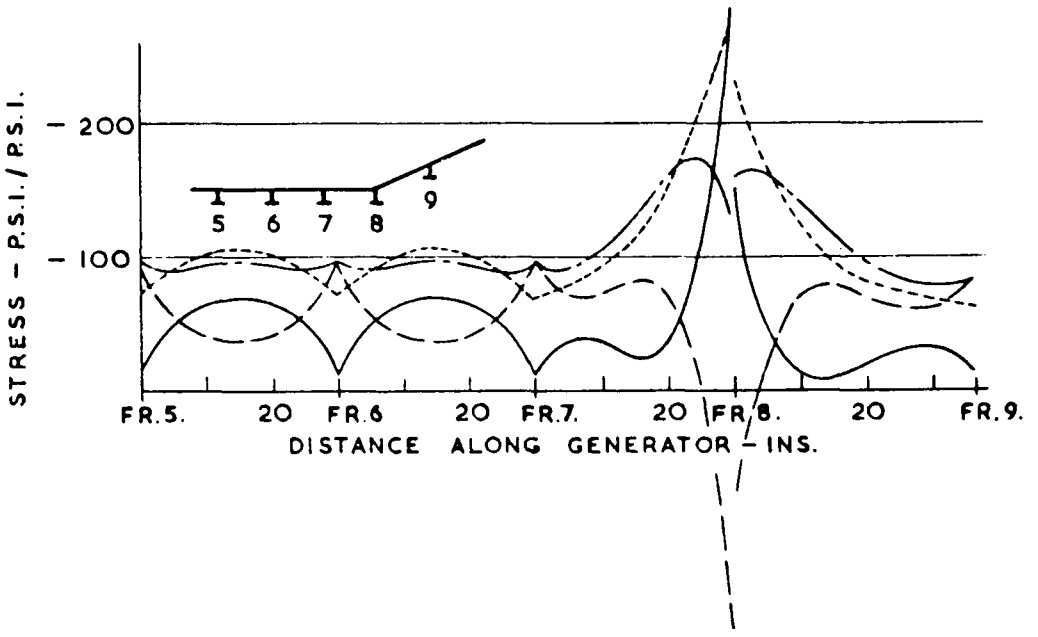


*(b) Stresses near cone-cylinder junction.*

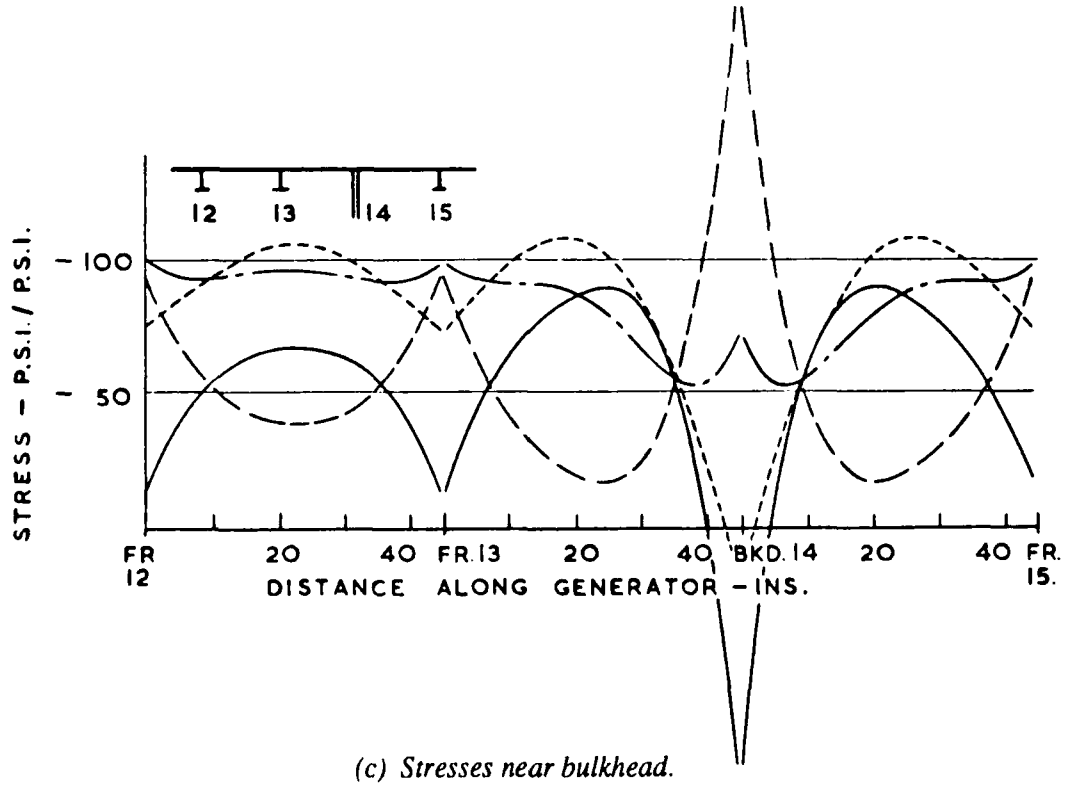


*(c) Stresses near bulkhead.*

*Figure 7 (continued)*

(i) The stress levels vary periodically on passing from frame to frame.

(ii) The average longitudinal stress (i.e. average of stresses at interior and exterior surfaces) is approximately $\sigma_z = -pR/2h$ and the average circumferential stress is slightly less than $\sigma_\theta = -pR/h$ due to the stiffening effect of the rings ($\sigma_z$ and $\sigma_\theta$ are the stresses for a uniform cylinder given in Section 3. For a cylinder of radius 3 m and thickness 25 mm, $\sigma_z = -60$ MPa and $\sigma_\theta = -120$ MPa at 100 m depth).

(iii) Stresses vary in the longitudinal direction due to shell bending over the rings. The longitudinal stresses show the most variation, with the external and internal surface stresses mirror images of each other (reflected in the mean stress -pR/2h).

(iv) The circumferential stresses are similar at both surfaces, but mimic the variation of the corresponding longitudinal stress because of the Poisson effect.

Bulkheads and section transitions may cause large stress concentrations, although their influence does not spread very far into the adjacent structure. The stress concentrations occur because of differences in the radial stiffness of adjacent sections, and the resultant bending of the plating to accommodate the different deflections under external pressure. The stress concentrations at:

(i) A dome-cylinder junction
(ii) A cone-cylinder junction
(iii) A bulkhead in a cylindrical section

are shown in Figure 7(a), (b) and (c) respectively. The stress concentration at the dome-cylinder junction is very small compared with the other two.

The stress concentration factors can be reduced by curved transitions and other methods of matching the radial stiffness across the structural discontinuity. This may be done by locally modifying the shell thickness, frame depth or frame spacing.

## *5.3 Symbols*

The symbols listed below are used in the calculation of the hull plating stresses in following sections of this report. Some are illustrated in Figure 8.

| | |
|---|---|
| $\theta$ | circumferential coordinate |
| $z$ | axial coordinate (measured from mid-way between frames) |
| $r$ | radial coordinate (measured from cylinder axis) |
| $\rho$ | radial coordinate (measured from shell mid-thickness) |
| $u$ | axial displacement of mid-surface of shell |
| $v$ | circumferential displacement |
| $w$ | radial displacement (positive outwards) |
| $R$ | shell radius at mid thickness |
| $R_f$ | radius of centroid of ring stiffener |

| | |
|---|---|
| h | shell thickness |
| $L_f$ | ring stiffener spacing |
| b | ring faying flange width |
| L | unsupported length of shell ($L = L_f - b$) |
| $A_f$ | cross sectional area of ring stiffener |
| p | hydrostatic pressure (positive if external) |
| E | Young's modulus of shell and rings |
| $\nu$ | Poisson's ratio of shell and rings |
| $\sigma$ | stress |
| $\epsilon$ | strain |
| M | bending moment |
| Q | radial shear force |
| N | membrane force (stress resultants) |
| I | $h^3 / [12 (1 - \nu^2)]$ |
| D | flexural rigidity of shell ($D = EI$) |
| $I_f$ | moment of inertia of ring stiffener |
| $\alpha$ | fourth root of $3(1 - \nu^2) / (hR)^2$ |
| K | frame rigidity constant (total load on ring per unit radial deflection per unit circumferential length) |

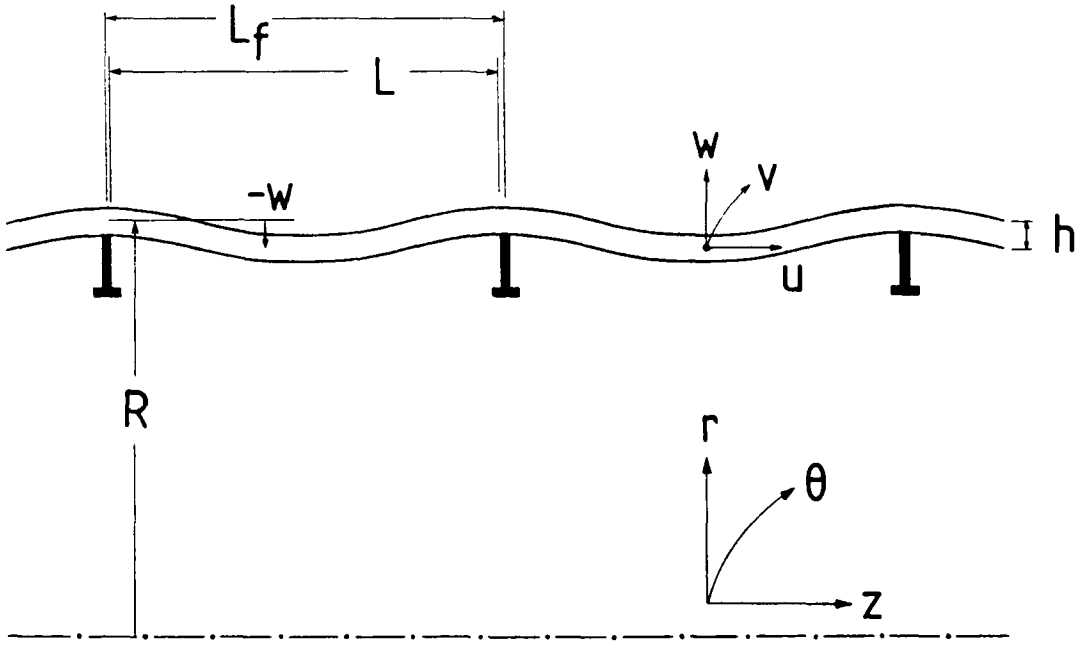


*Figure 8: Symbols used to describe the geometry of uniformly-framed, ring-stiffened cylinders.*

## 5.4 *Uniformly Framed Cylinders*

The first complete stress analysis of a perfectly circular, transversely-framed cylinder was carried out by von Sanden and Gunther (1920, 1921). It is the basis of subsequent analytical solutions of the problem, both in the formulation of the differential equation and in the method of solution. They found that stresses in the shell plating are strongly influenced by ring-stiffener cross section and spacing.

The mathematical analysis considers an element of the shell consisting of a longitudinal strip from one stiffener to the next. The strip is analysed as a beam supported by contiguous shell elements, with its ends resting on an elastic foundation (the stiffening rings). Therefore the governing differential equation is similar to that for pure bending of a beam:

$$EI_x (d^2w/dz^2) = M \qquad (8)$$

The full derivation of the differential equation is given by Timoshenko and Woinowsky-Krieger (1959), for example.

A preliminary analysis was carried out ignoring the effect of pressure on the end closures of the cylinder, allowing free movement in the axial direction so $\sigma_z = 0$. The resulting boundary value problem and its solution are presented in Appendix 1. Two of the boundary conditions are obtained from symmetry considerations, and the third is obtained by considering the radial force balance at the stiffeners (external pressure plus shell shear force equals ring reaction force).

Von Sanden and Gunther also modified their solution to partially take end pressure into account. The changes are listed in Appendix 2. The longitudinal membrane stress becomes -pR/2h but other stresses are unchanged.

Viterbo (1930) pointed out that if $A_f$ is set to zero (i.e. a cylinder without ring stiffeners), the von Sanden-Gunther solution predicts a shell load of less than p per unit area (the applied pressure). The inconsistency is removed by dividing the (radial) pressure into components $\rho v/2$ and $p - \rho v/2$, and noting that the $\rho v/2$ component together with the axial load due to end pressure produces (approximately) no deformation of the stiffening rings (see Young, 1989). This leads to a modification of the third boundary condition and a new solution as shown in Appendix 3.

Salerno and Pulos (1951) further refined the solution by incorporating the full effect of the end pressure. The Viterbo boundary conditions still apply but the differential equation includes a non-linear, beam-column term (Appendix 4). Solution of this problem is along the same lines as the von Sanden-Gunther solution (see also Moshaiov and Joelson, 1989) but it is more tedious and results in more complicated expressions for shell deflection and stresses. However it is regarded as the exact solution for a uniform, ring-stiffened cylinder under external hydrostatic pressure. Deflection and stresses are no longer linearly related to the pressure.

The process of solution of the complete Salerno-Pulos problem has been simplified for stresses at mid-bay (at $z = 0$, midway between the stiffeners) by the graphical solutions of Krenzke and Short (1959). Wilson (1956 a, b, c) used two methods to obtain accurate approximations to the Salerno-Pulos solutions. One method assumes that the shell deflection as a function of pressure takes the form of a power series in p. The other assumes a Fourier series form.

The power series (asymptotic) solution is described in Appendix 5. For various test cases studied by Wilson, the asymptotic solution is within 5% of the Salerno-Pulos solution. It is regarded as satisfactory provided the linear term $pw_1$ is much larger than the correction term $p^2w_2$ (where the total deflection is $w = pw_1 + p^2w_2$).

The Fourier series method (Appendix 6) allows another small refinement to the governing differential equation. In practice, only the first few terms in the Fourier series are required to obtain an accurate approximation to the full Salerno-Pulos solution. Wilson also used slightly modified expressions for the frame rigidity constant, K, and the shell stresses. The stress equations are based on simple elasticity equations for plane stress such as:

$$\sigma_{xx} = E(\epsilon_{xx} + \nu\epsilon_{yy}) / (1 - \nu^2) \qquad (9)$$

Wilson also considered the effects of factors such as out-of-circularity on shell stresses. These effects are considered in Section 5.10.

## *5.5 Computer Program for Uniformly Framed Cylinders*

A computer program has been written at MRL to implement the:

(i) Von Sanden and Gunther
(ii) Viterbo
(iii) Wilson power series
(iv) Wilson Fourier series

solutions for stresses in the shell of a uniformly framed cylinder subject to external pressure. Shell displacement and curvature, and longitudinal and circumferential stresses in the shell at mid-thickness and both surfaces are calculated (shell buckling is not considered).

## *5.6 Stress Concentrations due to Axisymmetric Structure*

To this point only uniformly-framed cylinders have been analysed. In this section, consideration is given to some departures from uniform framing such as bulkheads, heavy stiffeners, transitions (e.g. cylinder-cone junctions) and junction of a cylinder with end closures.

The analysis is based on that presented by Gill (1970) for infinite cylinders subject to edge loading. For asymmetric loading of a shell element of length dz and width r dθ the stress resultants are as shown in Figure 9 and the equilibrium equations are as follows:

$$
\left.
\begin{aligned}
& r\,(\partial N_z/\partial z) + (\partial N_{\theta z}/\partial \theta) + r p_z = 0 \\
& (\partial N_\theta/\partial \theta) + r(\partial N_{z\theta}/\partial z) - Q_\theta + r p_\theta = 0 \\
& (\partial Q_\theta/\partial \theta) + r(\partial Q_z/\partial z) + N_\theta - r p_r = 0 \\
& (\partial M_\theta/\partial \theta) + r(\partial M_{z\theta}/\partial z) - r Q_\theta = 0 \\
& r(\partial M_z/\partial z) + (\partial M_{\theta z}/\partial \theta) - r Q_z = 0 \\
& r N_{z\theta} - r N_{\theta z} + M_{\theta z} = 0
\end{aligned}
\right\} \qquad (10)
$$

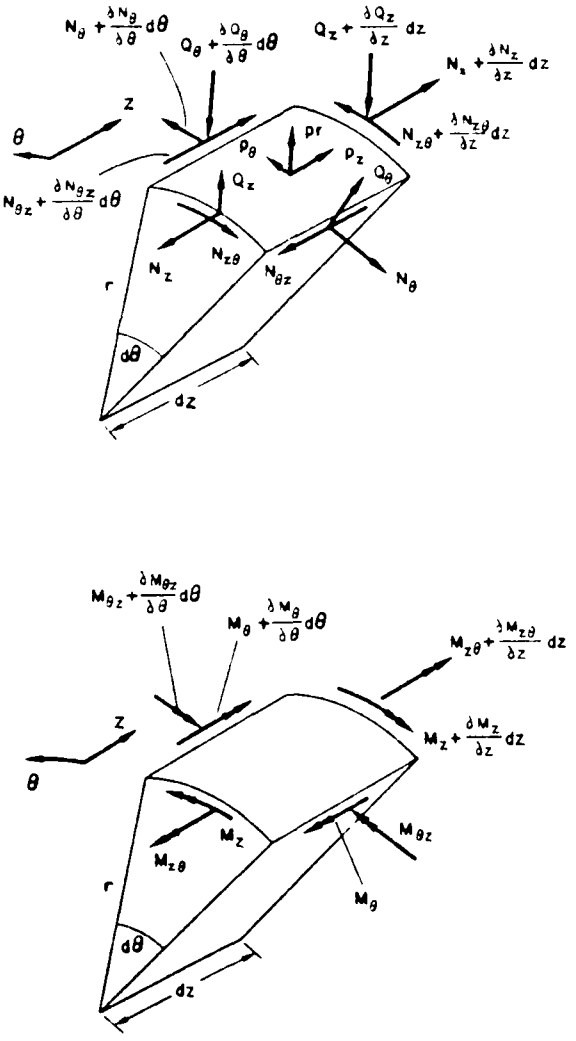


*Figure 9: Stress resultants for asymmetric loading of an element dz × r dθ of a cylindrical shell.*

If the loading is axially symmetric (e.g. hydrostatic pressure), $p_\theta = 0$ and $N_{z\theta} = N_{\theta z} = M_{z\theta} = Q_\theta = 0$ so the equations reduce to:

$$\left.\begin{aligned} &(dN_z/dz) + p_z = 0 \\ &r\,(dQ_z/dz) + N_\theta - rp_r = 0 \\ &(dM_z/dz) - Q_z = 0 \end{aligned}\right\} \qquad (11)$$

For linear elastic material, and considering only shear ($Q_z$) and moment ($M_z$) edge loading (at $z$ = const.), the following simplifications apply:

$$\left.\begin{aligned} &p_r = p_z = 0 \\ &N_z = 0 \\ &N_\theta = Ehw/r \\ &M_z = D\,(d^2w/dz^2) \end{aligned}\right\} \qquad (12)$$

Substituting into the equilibrium equations (11) gives:

$$EI\,(d^4w/dz^4) + Ehw/R^2 = 0 \qquad (13)$$

This is the differential equation for a circular cylinder subjected to rotationally symmetric edge loading. It is equivalent to the initial Van Sanden and Gunther analysis with p = 0 (Appendix 1). The general solution is as in Appendix 1 with p = 0, or equivalently, and more conveniently in this case, is:

$$\begin{aligned} w = {} & \exp(\alpha z)\,[k_1 \cos(\alpha z) + k_2 \sin(\alpha z)] \\ & + \exp(-\alpha z)\,[k_3 \cos(\alpha z) + k_4 \sin(\alpha z)] \end{aligned} \qquad (14)$$

Consider a semi-infinite cylinder subjected to symmetric edge loadings $M_o$ and $Q_o$ at $z = 0$ (Figure 10). Because the effect of the edge loading must decay with increasing $z$, the coefficients $k_1$ and $k_2$ are zero. The coefficients $k_3$ and $k_4$ are determined by the boundary conditions at the free edge ($z = 0$).

Due to the exponential term, the radial deflection $w$ is significant only for $\alpha z < \pi$. For a 5 m diameter steel pressure vessel with walls 25 mm thick, this condition is equivalent to $z <$ 0.71 m (this distance is of the order of the spacing of submarine hull ring stiffeners). Thus the effects of the edge loading are significant only in one bay.

This is an important simplification in the analysis of hull stresses. A stress concentration such as a bulkhead or heavy stiffener imposes radially symmetric loads on the edge of the adjacent hull cylinder. The resulting deflections will usually only be significant in the hull plating between the stress concentration and the nearest stiffening ring. However,

if two stress concentration points are located closer together than $\pi/\alpha$, then the $\exp(\alpha z)$ term in equation (14) cannot be deleted and the interference between the two must be considered.

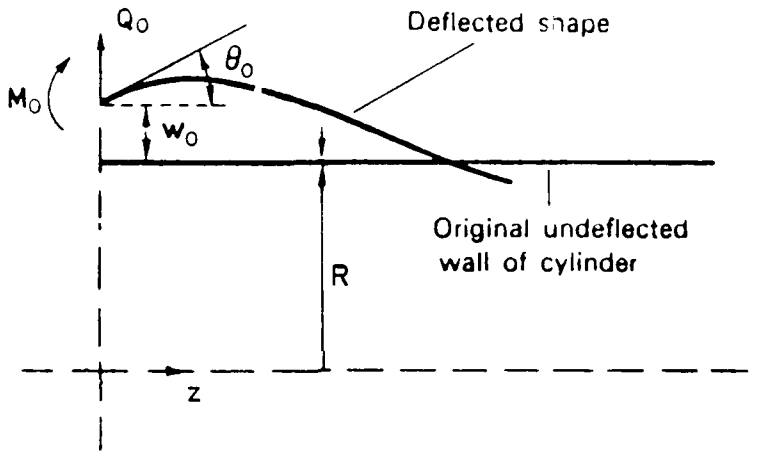


*Figure 10: Edge loadings $Q_o$ and $M_o$ on a cylindrical shell produce deflection $w_o$ and slope tan ($\theta_o$) (from Gill, 1970).*

Table 1 (Gill, 1970) shows solutions of equation (14) for various boundary conditions (edge loadings). In the case of a submarine hull, the deflections due to hydrostatic pressure must be added to obtain the complete solution. This process is described for various types of stress concentrator in the following sections.

### *5.6.1 Cylinder-Hemisphere Junction*

A well-studied situation giving rise to a stress concentration is the closure of a cylinder with a hemispherical cap. In the case of equal shell thicknesses, the stresses and radial displacements of simple cylindrical and spherical shells due to external pressure are:

***Table 1:*** *Edge Solutions for a Long Cylindrical Shell*

| End Condition | Deflection, w | Slope, dw/dz / Curvature, $d^2w/dz^2$ | M = EI $(d^2w/dz^2)$ / Q = dM/dz | Required Edge Deflection or Edge Forces |
|---|---|---|---|---|
|   | $(2R^2\alpha/Eh)\ Q_oD(\alpha z)$ | $(-2R^2\alpha^2/Eh)Q_o\ A(\alpha z)$ / $(4R^2\alpha^3/Eh)Q_o\ B(\alpha z)$ | $(Q_o/\alpha)\ B(\alpha z)$ / $Q_o\ C(\alpha z)$ | $w_o = (2R^2\alpha/Eh)Q_o$ / $\theta_o = (-2R^2\alpha^2/Eh)\ Q_o$ |
|   | $(2R^2\alpha^2/Eh)\ M_oC(\alpha z)$ | $(-4R^2\alpha^3/Eh)M_o\ D(\alpha z)$ / $(4R^2\alpha^4/Eh)M_o\ A(\alpha z)$ | $M_o\ A(\alpha z)$ / $-2\alpha M_o\ B(\alpha z)$ | $w_o = (2R^2\alpha^2/Eh)\ M_o$ / $\theta_o = (-4R^2\alpha^3/Eh)\ M_o$ |
| 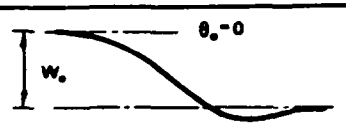  | $w_oA\ (\alpha z)$ | $-2\alpha w_o\ B(\alpha z)$ / $-2\alpha^2w_o\ C(\alpha z)$ | $(-Eh/2R^2\alpha^2)w_o\ C(\alpha z)$ / $(Eh/R^2\alpha)w_o\ D(\alpha z)$ | $Q_o = 4\alpha^3Dw_o$ / $M_o = -2\alpha^2Dw_o$ |
| 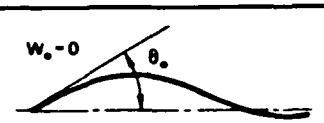  | $(\theta_o/\alpha)\ B(\alpha z)$ | $-\theta_o\ C(\alpha z)$ / $-2\alpha\theta_o\ D(\alpha z)$ | $(-Eh/2R^2\alpha^3)\ \theta_o\ D(\alpha z)$ / $(Eh/2R^2\alpha^2)\theta_o\ A(\alpha z)$ | $Q_o = 2\alpha^2D\theta_o$ / $M_o = -2\alpha D\theta_o$ |

$A(\alpha z) = \exp(-\alpha z)(\cos \alpha z + \sin \alpha z)$
$B(\alpha z) = \exp(-\alpha z) \sin \alpha z$
$C(\alpha z) = \exp(-\alpha z)(\cos \alpha z - \sin \alpha z)$
$D(\alpha z) = \exp(-\alpha z) \cos \alpha z$
M is the longitudinal bending moment per unit width
Q is the shear force per unit width

Cylinder: $\sigma_\theta = - pR / h$ (1)

$\sigma_z = - pR / 2h$ (3)

$w_1 = - pR^2 (2 - \nu) / 2Eh$ (4)

Sphere: $\sigma_\theta = \sigma_\psi = - pR / 2h$ (15)

$\delta_1 = - pR^2 (1 - \nu) / 2Eh$ (16)

The deflections are not equal, so equal and opposite shear forces and bending moments must exist at a junction between cylinder and hemisphere in order to maintain continuity. The edge loading solutions for a cylinder shown in Table 1 and similar results for a sphere shown in Table 2 allow the shear force $Q_o$ and bending moment $M_o$ to be obtained by equating the displacements $w_o$ and $\delta_o$ and slopes dw/dz and $\tan(\theta_o)$ on either side of the junction. The procedure for calculating the total stress in the cylindrical and hemispherical shell involves superposition of the membrane and edge bending solutions, and is known as "discontinuity analysis" (Cloud, 1970).

Gill (1970) gives details of the calculations. Referring to Figure 11 and Tables 1 and 2 (noting $\beta = \pi/2$ in this case), the edge displacements and slopes due to edge forces $Q_o$ and $M_o$ are:

Cylinder: $w_o = 2Q_o \alpha R^2 / Eh + 2M_o \alpha^2 R^2 / Eh$ (17)

$\theta_o = -2Q_o \alpha^2 R^2 / Eh - 4M_o \alpha^3 R^2 / Eh$ (18)

Sphere: $\delta_o = 2M_o \alpha^2 R^2 / Eh - 2Q_o \alpha R^2 / Eh$ (19)

$\theta_o = 4M_o \alpha^3 R^2 / Eh - 2Q_o \alpha^2 R^2 / Eh$ (20)

Matching the deflections and slopes across the discontinuity due to the combination of hydrostatic pressure with the edge loadings therefore requires:

$$w_1 + w_o = \delta_1 + \delta_o \quad (21)$$

$$\theta_o = -2Q_o \alpha^2 R^2/Eh - 4M_o \alpha^3 R^2/Eh = 4M_o \alpha^3 R^2/Eh - 2Q_o \alpha^2 R^2/Eh \quad (22)$$

These allow $M_o$ and $Q_o$ to be obtained:

$M_o = 0$ (23)

$Q_o = p / 8\alpha$ (24)

**Table 2 Edge Bending Solutions for a Spherical Shell ($\phi > 30°$)**

**Geometry**

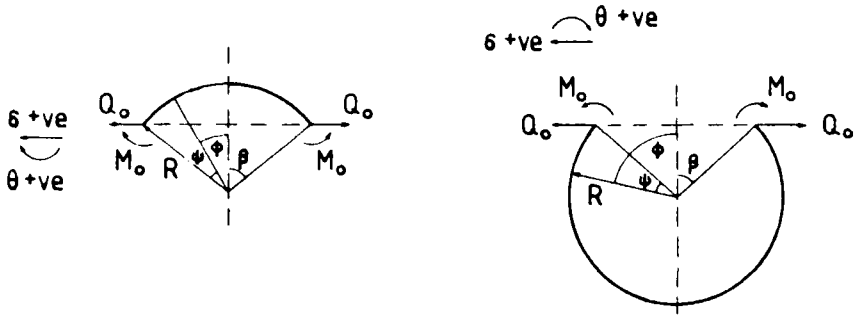


| **Stress Resultant** | | |
|---|---|---|
| $Q_\phi$ | $A \exp(-\alpha R\psi) \sin(\alpha R\psi + \gamma)$ | $A \exp(-\alpha R\psi) \sin(\alpha R\psi + \gamma)$ |
| $N_\phi$ | $- Q_\phi \cot(\beta - \psi)$ | $- Q_\phi \cot(\beta + \psi)$ |
| $N_\theta$ | $- \sqrt{2}\alpha R\, A \exp(-\alpha R\psi) \sin(\alpha R\psi+\gamma-\pi/1)$ | $+ \sqrt{2}\alpha R\, A \exp(-\alpha R\psi) \sin(\alpha R\psi+\gamma-\pi/4)$ |
| $M_\phi$ | $+(1/\sqrt{2}\alpha)\, A \exp(-\alpha R\Psi) \sin(\alpha R\psi+\gamma+\pi/4)$ | $-(1/\sqrt{2}\alpha)\, A \exp(-\alpha R\psi) \sin(\alpha R\psi+\gamma+\pi/4)$ |
| $M_\theta$ | $\nu M_\phi$ | $\nu M_\phi$ |
| **Rotation** | | |
| $\theta$ | $(2\alpha^2R^2/Eh)\, A \exp(-\alpha R\psi) \cos(\alpha R\psi+\gamma)$ | $(2\alpha^2R^2/Eh)\, A \exp(-\alpha R\psi) \cos(\alpha R\psi+\gamma)$ |
| **Constants for Boundary Conditions*** | | |
| $M_o$ only | $A = 2\alpha M_o \quad \gamma = 0$ | $A = -2\alpha M_o \quad \gamma = 0$ |
| $Q_o$ only | $A = \sqrt{2}\, Q_o \sin\beta \quad \gamma = -\pi/4$ | $A = -\sqrt{2}\, Q_o \sin\beta \quad \gamma = -\pi/4$ |
| **Edge Rotation** | | |
| $\theta_o$ | $(4\alpha^3R^2/Eh)M_o + (2\alpha^2R^2/Eh)Q_o \sin\beta$ | $-4(\alpha^3R^2/Eh)M_o - (2\alpha^2R^2/Eh)Q_o \sin\beta$ |
| **Edge Deflection** | | |
| $\delta_o$ | $(2\alpha^2R^2/Eh)M_o \sin\beta + (2\alpha R^2/Eh)Q_o \sin^2\beta$ | $(2\alpha^2R^2/Eh)M_o \sin\beta + (2\alpha R^2/Eh)Q_o \sin^2\beta$ |

* The values of A and $\gamma$ are found for $M_o$ and $Q_o$ applied separately and added before substituting into the expressions for the stress resultants and rotation.

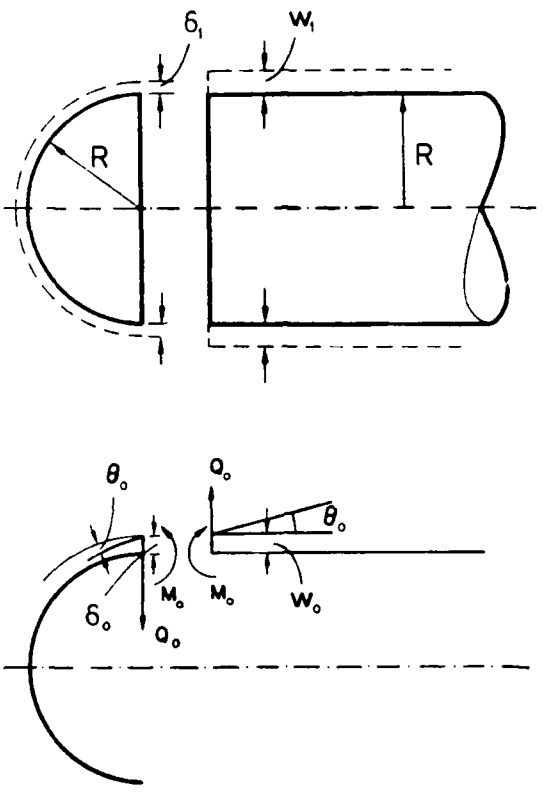


(a)

(b)

*Figure 11: Deflections and slopes at a hemisphere-cylinder junction (a) due to pressure and (b) due to edge loadings $Q_o$ and $M_o$.*

The total deflections, due to $Q_o$ (obtained from Tables 1 and 2) combined with those due to hydrostatic pressure are:

$$w + w_1 = (pR^2/4Eh)\exp(-\alpha z)\cos(\alpha z) - pR^2(2-\nu)/2Eh \quad (25)$$

$$\delta + \delta_1 = -(pR^2/4Eh)\exp(-R\alpha\psi)\cos(R\alpha\psi)\cos(\psi) - pR^2(1-\nu)/2Eh \quad (26)$$

Knowing the deflections, the stresses can now be calculated as in Appendices 1 to 6. Results are shown in Figure 12 (Gill, 1970). Note that the bending of the sphere and cylinder near the junction increases the longitudinal/meridional stress from -pR/2h to about -1.3 pR/2h at one surface (and reduces it to -0.7 pR/2h at the other). The hemisphere is stiffer than the cylinder in the radial direction, so the radial deflection of the cylinder is reduced at the junction. This leads to reduced circumferential stress at that point for the cylinder (and increased stress for the sphere). Bending has a relatively small effect on the circumferential stress.

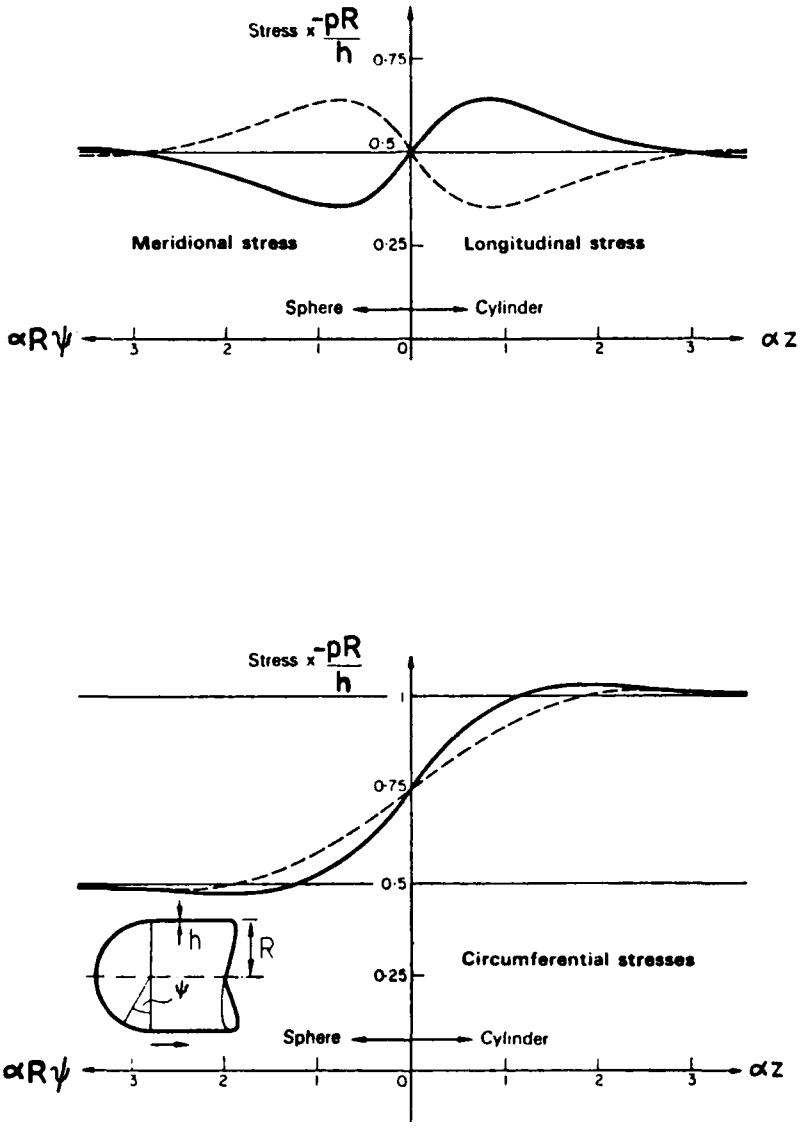


*Figure 12: Stresses at the junction of hemispherical and cylindrical shells under external hydrostatic pressure (from Gill, 1970. See also Figure 7).*

- - - - - - - - - *Inner surface*

——————— *Outer surface*

### 5.6.2 *Flat Plate End Closure*

Although the hemispherical end closure is efficient from the point of view of limiting stress concentrations in a pressure vessel, it is rather difficult to fabricate, especially for large vessels. Flat plate end closures as found in the Type 471 submarine design[1] greatly simplify construction. The inward dishing of the plate under pressure gives rise to a large stress concentration at the junction with the hull cylinder. However the junction can be strengthened sufficiently to compensate for this with slight weight penalty.

A hemispherical end carries hydrostatic pressure entirely as a membrane except near the junction. In the case of a flat closure the pressure is carried entirely by means of bending stresses. Membrane stresses become important only after significant deflection occurs. The theory of symmetric bending of circular plates is developed by Timoshenko and Woinowsky-Krieger (1959). Referring to Figure 13 and considering only axially symmetric loads, the principal curvatures of the circular plate are:

$$1/r_n = -(d^2u/dr^2) = (d\phi/dr) \tag{27}$$

$$1/r_\theta = -(du/dr)/r = \phi/r \tag{28}$$

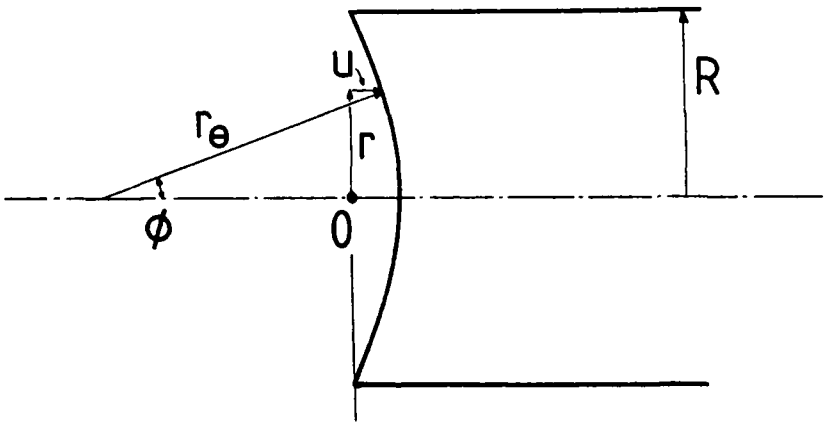


*Figure 13: Notation for the analysis of symmetric bending of a circular plate.*

1 The Type 471 end closures are not simple flat plates because of adjacent bulkheads, tanks and torpedo tubes in front of the forward closure, and structure supporting the propellor shaft behind the after closure. The closures themselves also have a stiffening grillage.

The moments (per unit length in the plane of the plate) are:

$$M_r = D\,(1/r_n + \nu/r_\theta) = D\,[(d\phi/dr) + \nu\phi/r] \tag{29}$$

$$M_\theta = D\,(\nu/r_n + 1/r_\theta) = D\,[\nu\,(d\phi/dr) + \phi/r] \tag{30}$$

Considering the torque on a small element of the plate about a tangential axis due to these moments and the axially symmetric shear force Q (per unit length), the equilibrium condition is:

$$M_r + (dM_r/dr)r - M_\theta + Qr = 0 \tag{31}$$

$$(d^3u/dr^3) + (d^2u/dr^2) / r - (du/dr) / r^2 = Q/D \tag{32}$$

In the case of hydrostatic pressure loading, Q = pr/2 and the solution of the differential equation is:

$$u = pr^4/64D + c_1r^2/4 + c_2\log(r) + c_3 \tag{33}$$

where the constants $c_1$, $c_2$ and $c_3$ are determined by the boundary conditions. Taking u = 0 at the circumference of the plate (r = R) and noting the symmetry requirement (du/dr) = 0 at r = 0 we have:

$$c_2 = 0 \tag{34}$$

$$c_3 = -(pR^4 / 64D + c_1R^2 / 4) \tag{35}$$

$$u = p(r^4 - R^4) / 64D + c_1(r^2 - R^2) / 4 \tag{36}$$

For a plate loaded with pressure alone, $M_r = 0$ at r = R (free edge) and:

$$u = (p/64D)\,(R^2 - r^2)\,[R^2\,(5 + \nu) / (1 + \nu) - r^2] \tag{37}$$

For a plate loaded with a radial edge bending moment $M_r = M_o$ (at r = R) in addition to the pressure:

$$u = (p/64D)\,(R^2 - r^2)\,[R^2\,(5 + \nu) / (1 + \nu) - r^2] + M_o(R^2 - r^2) / 2D(1 + \nu) \tag{38}$$

The discontinuity stresses for a flat plate closure of a cylinder can now be calculated in the same way as for a hemispherical cap by equating deflections and slopes across the junction. The forces required to maintain continuity are shown in Figure 14 (Cloud, 1970). The response to pressure and edge moment have already been considered. The shear force F at the edge of the plate is required to balance the pressure load (F = pR/2) and is independent of the deflection at the junction. For plates of practical proportions, the effect of the in-plane

force $Q_o$ can be neglected (the plate is effectively rigid and does not deflect radially, $w_p = 0$). However F and $Q_o$ must still be considered as far as the cylinder is concerned.

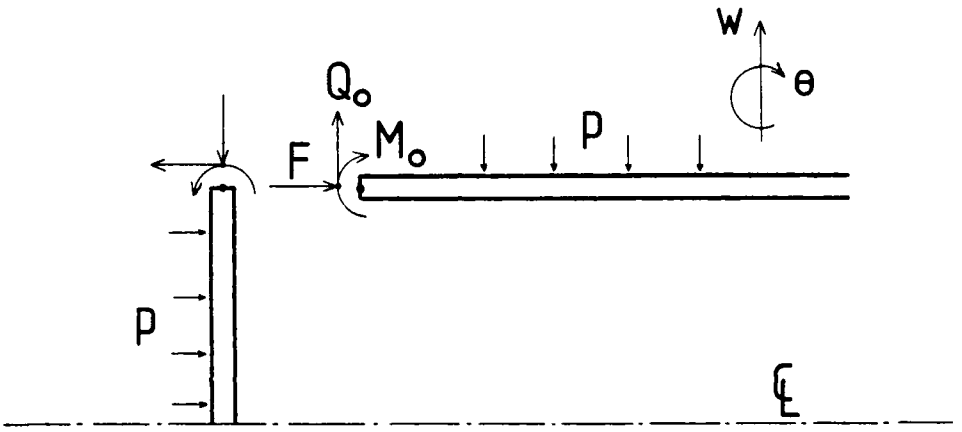


*Figure 14: Discontinuity analysis of the junction between a cylindrical shell and a flat plate end closure under external hydrostatic pressure. Forces F and $Q_o$, and moment $M_o$ act at the junction.*

Using equations (4), (17) and (18) for the slopes and deflections of the cylinder, and the results above for the plate, the continuity conditions at the junction are:

$$w_p = 0 = w_o + w_1 = 2Q_o\alpha R^2/Eh + 2M_o\alpha^2R^2/Eh - pR^2(2 - \nu) / 2Eh \qquad (39)$$

(Note here that the term involving $\nu$ takes the end force F on the cylinder into account.)

$$\theta_p = (du/dr)_{r=R} = \theta_o = (dw/dz)_{z=0} \qquad (40)$$

$$pR^3/8D\,(1 + \nu) + M_oR/D\,(1 + \nu) = -2Q_o\alpha^2R^2/Eh - 4M_o\alpha^3R^2/Eh \qquad (41)$$

Solving for $M_o$ and $Q_o$ assuming E and $\nu$ are the same for the cylinder and the plate:

$$M_o = - p [R^3\alpha^3H^3 + (2 - \nu)(1 + \nu)] / 4\alpha^2 (1 + \nu + 2R\alpha H^3) \quad (42)$$

$$Q_o = p [R^3\alpha^3H^3 + 2 (2 - \nu)(1 + \nu + R\alpha H^3)] / 4\alpha(1 + \nu + 2R\alpha H^3) \quad (43)$$

where H is the cylinder:plate thickness ratio ($h_c/h_p$) and $\alpha$ refers to cylinder dimensions. The deflections in the plate can now be obtained using equation (38), and the stresses are found as follows (Timoshenko and Woinowsky-Krieger, 1959):

$$\sigma_r = 12cM_r / h^3 = Ec[(d^2u/dr^2) + \nu(du/dr) / r] \quad (44)$$

$$\sigma_\theta = 12cM_\theta / h^3 = Ec[\nu(d^2u/dr^2) + (du/dr) / r] \quad (45)$$

where c is the distance from the mid-thickness of the plate and ranges from $-h_p/2$ to $h_p/2$. The cylinder deflections and stresses due to the edge forces $Q_o$ and $M_o$ combined with the hydrostatic pressure are as shown below.

$$w = 2\alpha R^2 \exp(-\alpha z) [Q_o \cos(\alpha z) + \alpha M_o (\cos \alpha z - \sin \alpha z)] / Eh$$
$$- pR^2 (2 - \nu) / 2Eh \quad (46)$$

$$d^2w/dz^2 = 4\alpha^3R^2 \exp(-\alpha z) [Q_o \sin(\alpha z) + \alpha M_o (\cos \alpha z + \sin \alpha z)] / Eh \quad (47)$$

$$\sigma_z = - pR/2h - E\rho [\nu w/R^2 + (d^2w/dz^2)] / (1 - \nu^2) \quad (48)$$

$$\sigma_\theta = Ew/R - \nu pR/2h - E\rho [w/R^2 + \nu (d^2w/dz^2)] / (1 - \nu^2) \quad (49)$$

The deflections and stresses are illustrated in Figure 15. The flat plate closure causes a large stress concentration in the cylindrical shell adjacent to the junction because of the bending induced by the moment $M_o$. A lighter end plate deflects more under pressure, imposes a larger $M_o$ on the cylinder, and results in larger stresses in the cylinder. The stresses in the end plate itself are small in comparison to those in the cylinder. A more detailed treatment of this problem is given by Watts and Lang (1982). Uddin (1987) considers the case of large deformations. Harvey (1985) considers grillage and ring reinforcement of the flat plate.

From the point of view of fatigue, it can be seen that the flat plate closure not only causes a stress concentration. It also causes the stresses near the outer surface of the cylindrical shell to become tensile near the junction. In fatigue, only tensile stresses are damaging (compressive applied stresses may also be damaging in the presence of tensile residual stresses).

A simple flat plate end closure must be very thick compared with a hemispherical end closure (or be reinforced). An alternative would be to thicken the cylindrical shell plating near the junction, in order to reduce the bending stresses.

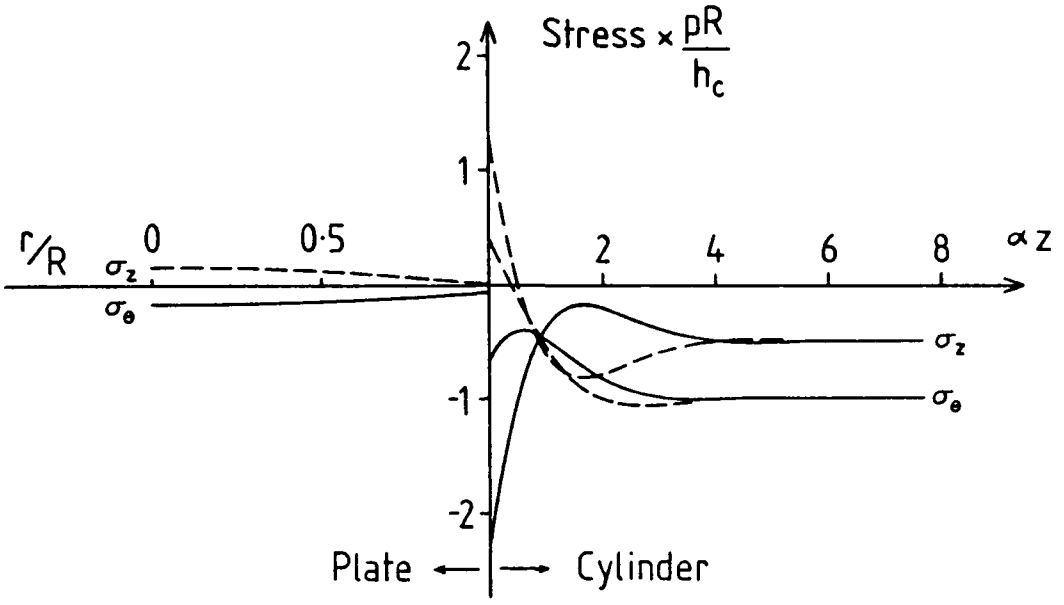


*(a) Circumferential ($\sigma_\theta$) and radial/longitudinal ($\sigma_r$ / $\sigma_z$) stresses for plate thickness 500 mm.*

———— *Inner surface*
– – – – – – – – *Outer surface*

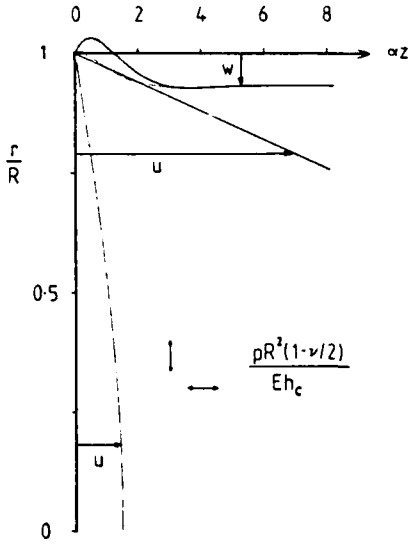


*(b) Deflections of cylinder (w) and plate (u).*

———— *plate 200 mm thick*
– – – – – – – – *plate 500 mm thick*

*Figure 15: Stresses and deflections for a cylindrical shell (radius 3 m, thickness 25 mm) with a flat plate end closure (thickness 200 mm or 500 mm) subjected to external hydrostatic pressure.*

### 5.6.3 *Bulkhead or Heavy Stiffening Ring*

The stress concentration due to a bulkhead or heavy stiffening ring may also be obtained by applying the edge loading formulas in Table 1. Considering an isolated stiffening ring in an infinite cylindrical shell, symmetry requires $\theta_o = 0$ (Figure 10) at the location of the stiffener. This situation is covered by Case 3 in Table 1 (and also in Table 29 of Young, 1989).

The edge force, $Q_o$, of interest here is the difference between the reaction force of a normal stiffening ring, and the reaction force of the bulkhead or heavy stiffening ring. The stress concentration due to the bulkhead or heavy stiffener can then be obtained by superposition with the solution for the uniformly framed cylinder.

The outward shear force per unit circumferential length, $Q_o$, applied to the hull plating by a standard stiffening ring is:

$$Q = - K\omega_{z=0} \tag{50}$$

(The symbol $\omega$ refers to deflection of a cylinder without a bulkhead and the symbol $w$ to that of a cylinder with a bulkhead). In this case the coordinate origin has been shifted to the location of the stiffening ring to simplify the algebra (in Appendices 1 to 6 the stiffeners are at $\pm L/2$). Thus $\omega_{z=0}$ is the deflection at the stiffening ring (positive outwards). The corresponding force due to a bulkhead or heavy frame is:

$$Q^1 = - K_H (\omega_{z=0} + w_o) \tag{51}$$

where the symbols are defined as shown in Figure 16. $w_o$ is defined in this way to be compatible with Table 1. Quantities, w, $\omega$ and $w_o$ are all positive in the outward direction, so w and $\omega$ are typically negative for external hydrostatic loading.

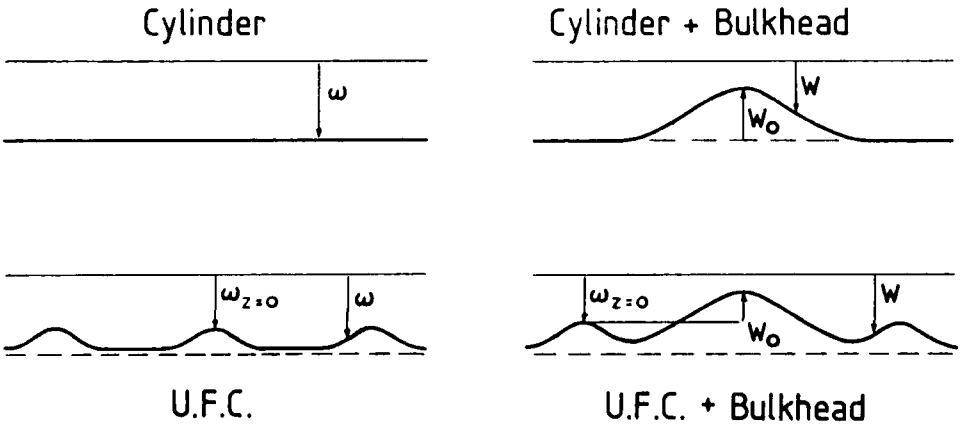


*Figure 16: Deflections of a simple cylindrical shell and a uniformly framed cylinder with and without a bulkhead.*

The required edge force is therefore:

$$Q_o = Q^I - Q$$

$$= (K - K_H)\,\omega_{z=0} - K_H\,w_o \qquad (52)$$

From Table 1 we have another expression for $Q_o$:

$$Q_o = Eh\,w_o / R^2\alpha \qquad (53)$$

which allows the following solution for $w_o$:

$$w_o = (K - K_H)\,\omega_{z=0} / (K_H + Eh/R^2\alpha) \qquad (54)$$

Again using Table 1 for the deflection of the stiffener due to the bulkhead or heavy stiffener, the total deflection is:

$$w = \omega + R^2\alpha\,(K - K_H)\,\omega_{z=0}\exp(-\alpha z)\,[\cos(\alpha z) + \sin(\alpha z)] / (R^2\alpha K_H + Eh) \qquad (55)$$

where $\omega$ is the deflection of the uniformly framed cylinder (or of the simple cylinder in the case $K = 0$).

For the case of a perfectly rigid bulkhead (i.e. $K_H = \infty$, $\omega_{z=0} = 0$ and $w_o = -\omega$) the hull plating displacement is:

$$w = \omega - \omega_{z=0}\exp(-\alpha z)\,[\cos(\alpha z) + \sin(\alpha z)] \qquad (56)$$

At the other extreme the bulkhead has the same stiffness as a normal stiffening ring ($K_H = K$) and $w = \omega$. Cases intermediate between these extremes are considered in Appendix 7.

The bulkhead or heavy frame introduces additional bending stresses compared with the uniformly framed cylinder (Short and Bart, 1959). For the worst case situation of a perfectly rigid bulkhead, the deflection and stresses due to the presence of the bulkhead are as shown in Figure 17. The stresses are calculated from the deflection as in Appendix 6 (and combined with existing stresses by superposition). The stresses in the cylinder are similar to those produced by the flat end closure (Figure 15(a) Section 5.6.2). Large tensile stresses occur at the outer surface of the shell plating.

### *5.6.4 Other Junctions*

Edge bending solutions have been obtained for a wide variety of shells of revolution by Hampe (1964). These include finite as well as infinite length cones, cylinders and spherical segments. Many of these results are listed by Baker et al. (1972) and summarized by Young (1989). The edge bending solutions allow deflections and stresses to be calculated for a wide variety of junctions between shells of revolution.

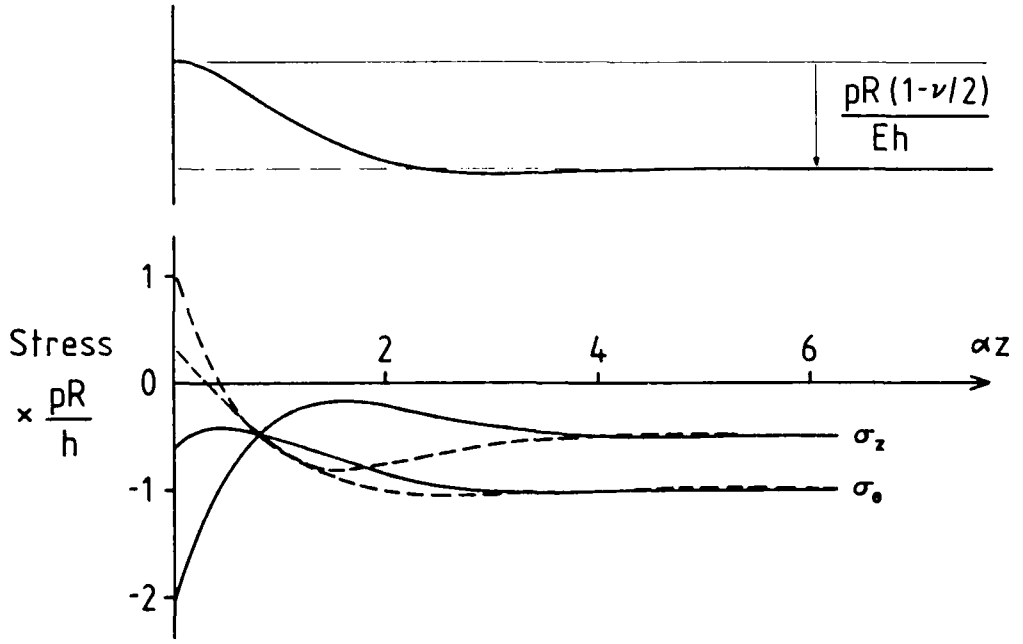


*Figure 17: Deflection and stresses for a cylindrical shell (radius 3 m, thickness 25 mm) adjacent to a rigid bulkhead.*

——————— *Stresses at inner surface*
— — — — — — — *Stresses at outer surface*

*See also Figures 7 and 15.*

Only one further junction will be considered here; the junction between cylindrical shells of unequal thickness. Proceeding as in Section 5.6.1, the deflection at the junction (see Figure 18) is.

$$w_1 + w_o = \delta_1 + \delta_o = w_o - pR^2 (2 - \nu) / 2Eh_2$$
$$= \delta_o - pR^2 (2 - \nu) / 2Eh_1 \qquad (57)$$

$$\delta_o = - 2R^2\alpha_1^2 M_o / Eh_1 - 2R^2\alpha_1 Q_o / Eh_1 \qquad (58)$$

$$w_o = -2R^2\alpha_2^2 M_o / Eh_2 + 2R^2\alpha_2 Q_o / Eh_2 \quad (59)$$

$$0_o = -4R^2\alpha_1^3 M_o / Eh_1 - 2R^2\alpha_1^2 Q_o / Eh_1 \quad (60)$$

$$= 4R^2\alpha_2^3 M_o / Eh_2 - 2R^2\alpha_2^2 Q_o / Eh_2$$

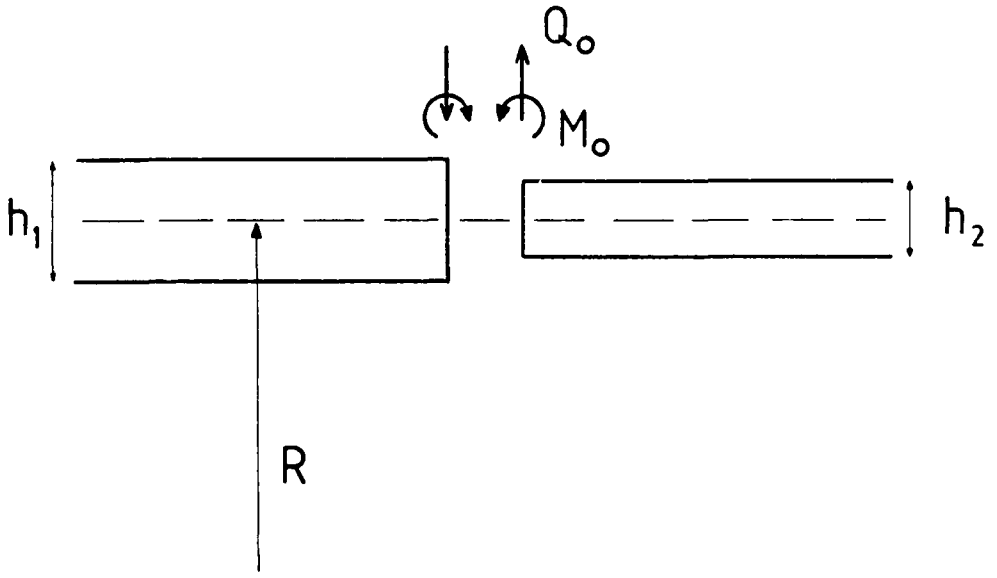


*Figure 18: Moment $M_o$ and shear force $Q_o$ required to maintain continuity of deflection and slope at the junction of two cylindrical shells of radius R.*

Solving the pair of equations (57) and (60) gives:

$$M_o = \frac{p(h_1 - h_2)(2 - \nu)(\alpha_1^2 h_2 - \alpha_2^2 h_1)}{4(\alpha_1^2 h_2 - \alpha_2^2 h_1)^2 - 8(\alpha_2^3 h_1 + \alpha_1^3 h_2)(\alpha_1 h_2 + \alpha_2 h_1)} \quad (61)$$

$$Q_o = -2M_o(\alpha_2^3 h_1 + \alpha_1^3 h_2) / (\alpha_1^2 h_2 - \alpha_2^2 h_1) \quad (62)$$

Again following the same procedure as in Section 5.6.1, the deflections and stresses are calculated from $M_o$ and $Q_o$. Results for a particular case are shown in Figure 19. It should be noted that shell theory does not take into account the stress concentration at the junction due to the geometrical change of section. Shell theory assumes uniform distribution of the membrane stress and linear variation of the bending stress through the thickness. The change of section leads to non-uniform distribution near the junction (see Section 5.11).

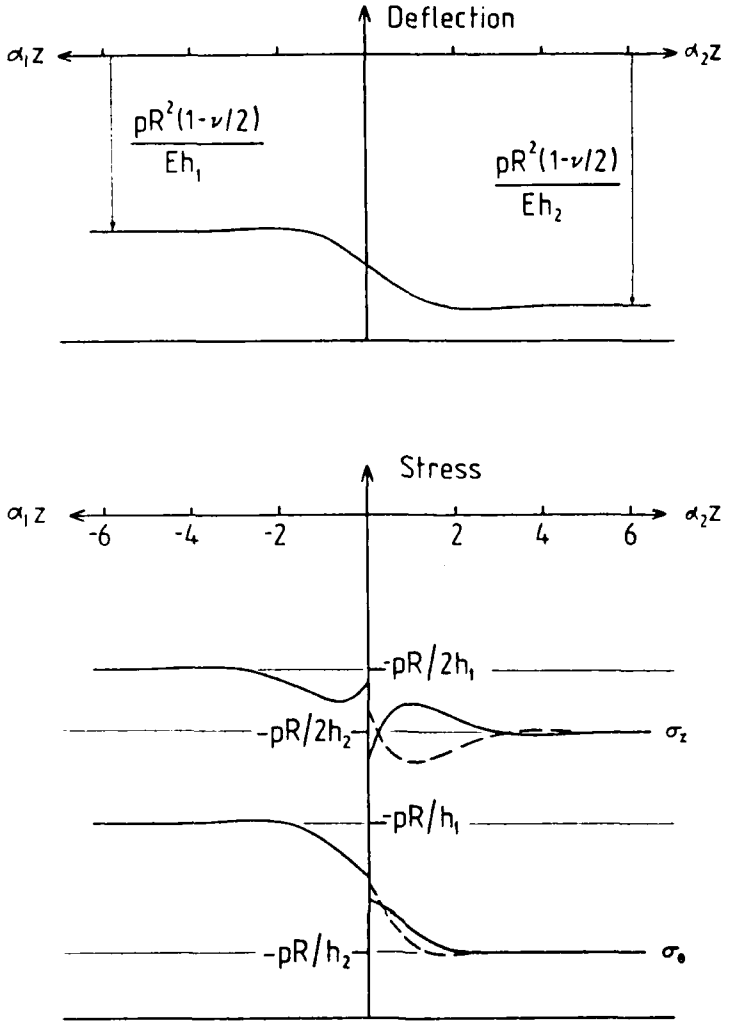


*Figure 19: Deflections and stresses near the junction of cylindrical shells of thickness $h_1$ = 50 mm and $h_2$ = 35 mm (R = 5 m, v = 0.3) as calculated from shell theory.*

——————— *Inner surface of shell*
— — — — — — *Outer surface of shell*

## *5.7 Non-Uniform Framing and More Complex Geometries*

Analytical solutions for submarine hull stresses are effectively limited to the simple uniformly framed cylinder (Section 5.4) and to relatively simple stress concentrators such as those considered in Section 5.6. Compared with the boundary value problem for the uniformly-framed cylinder, non-uniform framing adds to the number and complexity of boundary conditions to be satisfied. Analysing cylinders of non-uniform thickness, cones, domes, toroids and combinations of these forms is more difficult again because the governing differential equations are also more complex.

Kendrick (1964) lists the differential equations for a general axisymmetric shell. Similar equations from Gill (1970) have been presented in Section 5.6 and other forms may be found in the numerous textbooks on the subject (e.g. Gibson, 1980; Kraus, 1967; Timoshenko and Woinowsky-Krieger, 1959; Flügge, 1960; Baker et al., 1972; Novozhilov, 1959). While analytic solutions are available for special cases of interest (e.g. Young, 1989), computer solutions are much more general.

Axisymmetric stress analysis is much simpler than the general three dimensional problem, and computer codes have been written to capitalize on this simplicity. The programs available and their capabilities have been briefly reviewed by Bushnell (1974). His summary diagram is shown as Figure 20. A comprehensive review of the field is Bushnell (1985). In addition to static stress analysis, vibration and buckling of axisymmetric shells are encompassed by the programs. The effects of axisymmetric shape imperfections and residual stresses can also be investigated.

For dealing with parts of a submarine structure which are not axisymmetric, programs are available for general elastic-plastic shell analysis. Two of the better known ones are STAGS (Almroth et al., 1980) and ASAS (Atkins, 1982). General purpose finite element codes such as NASTRAN and ABAQUS have also been applied to solving design problems. Brebbia (1985) has surveyed a large number of finite element and boundary element packages. Their capabilities are summarized in Figure 21. These programs require considerable preparation and computing time. For this reason they are only applied to the analysis of structural details after the overall structure has been considered using an axisymmetric model.

## *5.8 Hull Attachments and Penetrations*

We move now to analysis of some non-axisymmetric features of a submarine hull structure. Local attachments such as the fin, and penetrations such as hatches are the most important of these. Such attachments and penetrations usually include local reinforcement of the hull cylinder in the form of thickened hull plating. A useful review of these aspects is given by Kitching (1970).

Loads due to small attachments and penetrations are called local loads because significant effects on the main cylindrical shell are usually confined to areas close to the attachment. Some typical types of "branches" are shown in Figure 22. Stress analysis of such branches has been confined to relatively simple geometries in which the boundary between shell and attachment has a relatively simple mathematical description. For cylindrical shells the boundaries considered are usually meridional or circumferential lines. For spherical shells the usual boundaries are circles. Analyses for more complex shapes are usually approximate and are often based on experimental observations utilizing the results for the basic cylinder and sphere intersections (or involve numerical analysis methods).

Under pressure loading, the change in shell geometry due to removing material for an opening or due to welding on additional reinforcing material leads to stress concentration. To minimize this, shape changes are usually gradual (e.g. rectangular pads on a cylinder have well-rounded corners). Bending stresses can be expected if the attachment is unsymmetrical with respect to the mid-plane of the shell plate. In the following sections, different types of hull penetrations and attachments are considered.

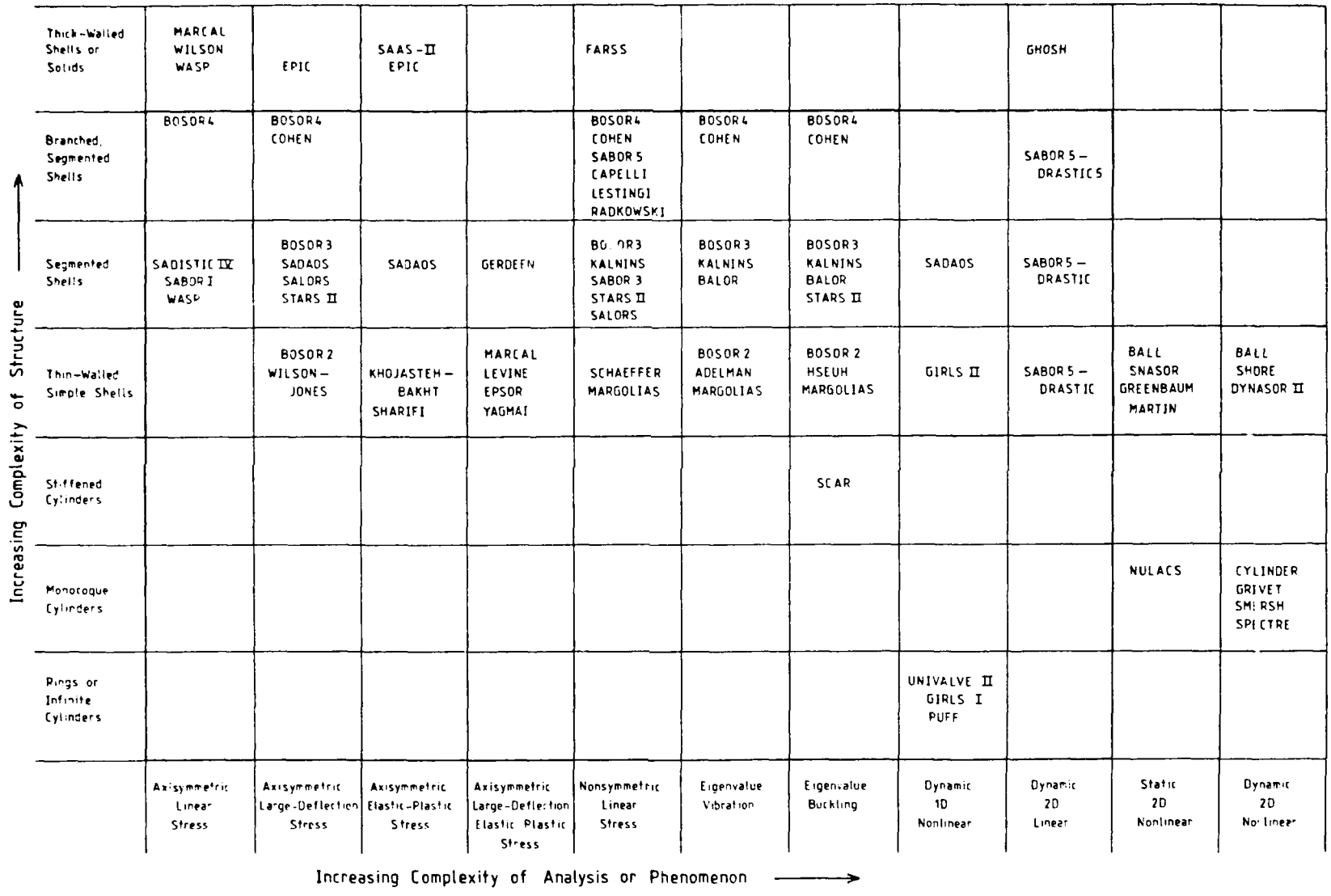


*Figure 20: Survey of computer codes for stress analysis of shells and solids of revolution (Bushnell, 1974)*

ELEMENT TYPE

| PROGRAM NAME | TRUSS AND BEAMS | 2-D SOLID | 3-D SOLID | AXIS SOLID | PLATE BENDING | SHELLS | BOUNDARY ELEMENTS | CRACK ELEMENTS | FLUID MECHANICS |
|---|---|---|---|---|---|---|---|---|---|
| ABAQUS | • | • | • | • | • | • | | • | • |
| ADINA | • | • | • | • | • | • | | • | • |
| ANSYS | • | • | • | • | • | • | | • | |
| APPLE-SAP | • | • | • | • | • | • | • | | |
| ASAS | • | • | • | • | • | • | | • | • |
| ASKA | • | • | • | • | • | • | | • | • |
| BEASY | | • | • | • | | | • | | |
| BERSAFE | • | • | • | • | • | • | | • | |
| CASTEM | • | • | • | • | • | • | | • | • |
| CASTOR | • | • | • | • | • | • | • | | • |
| CHALMFEM | • | • | • | • | • | • | • | | • |
| COMET-PR | | • | • | • | • | | | | |
| COSMOS | • | • | • | • | • | • | • | • | • |
| DART | | | | | | • | | | |
| DIAL | • | • | • | • | • | • | | • | |
| DIANA | • | • | • | • | • | • | | | |
| DREAM | • | | | | | | | | |
| FASOR | | | | | • | • | | | • |
| FELCO G | | • | | • | | | | | • |
| FENRIS | • | • | • | • | • | • | | | • |
| FIDAP | | | | | | | | | • |
| FLASH 2 | • | • | | • | • | • | | | |
| HIFINEL | • | • | • | • | | | | | |
| LAWPILE | • | | | | | | • | | |
| LISA | • | • | • | • | • | • | • | | |
| LUSAS | • | • | • | • | • | • | | • | |
| MARC | • | • | • | • | • | • | | | • |
| MBB-MAN-ICES-STRUDL | • | • | • | • | • | • | • | • | • |
| MICAS | • | • | • | • | • | • | • | | |
| MODEL | • | • | • | • | • | • | | • | • |
| MODULEF | • | • | • | • | • | • | | | • |
| MSC/NASTRAN | • | • | • | • | • | • | | • | • |
| PAFEC | • | • | • | • | • | • | • | • | |
| PDA/PATRAN-G | • | • | • | • | • | • | | | |
| PECET | | • | | | | • | | | |
| PREFEM & SERFEM | | • | | | • | | | | |
| RAFTS | • | | | | • | | • | | |
| SCIA | • | • | • | • | • | | | | • |
| SESAM-69 | • | • | • | | | • | | | |
| SET | • | • | • | • | • | • | • | | • |
| STARS | | | | • | | • | | | |
| STATIK | • | | | | | | | | |
| STDYNL | • | • | | | • | • | | | |
| THAFEM | | • | | • | | | | | |
| TITUS | • | • | • | • | • | • | • | • | • |

ANALYSIS CAPABILITIES

| PROGRAM NAME | STATIC ANALYSIS | TRANSIENT DYNAMICS | HARMONIC RESPONSE | BUCKLING | POST-BUCKLING | FRACTURE MECHANICS | HEAT TRANSFER |
|---|---|---|---|---|---|---|---|
| ABAQUS | • | • | • | • | • | • | • |
| ADINA | • | • | • | • | • | • | • |
| ANSYS | • | • | • | • | • | • | • |
| APPLE-SAP | • | • | • | | | | • |
| ASAS | • | | • | | | • | • |
| ASKA | • | • | • | • | | • | • |
| BEASY | • | | | | | | • |
| BERSAFE | • | • | • | | | • | • |
| CASTEM | • | • | | • | • | • | • |
| CASTOR | • | • | • | • | | • | • |
| CHALMFEM | • | • | • | • | | | • |
| COMET-PR | • | | | | | • | |
| COSMOS | • | • | • | • | • | • | • |
| DART | • | | • | | | | • |
| DIAL | • | • | • | • | • | | • |
| DIANA | • | • | • | • | • | | |
| DREAM | • | | | • | • | | |
| FASOR | • | | • | • | | | |
| FELCO G | • | • | | | | | • |
| FENRIS | • | • | • | • | • | | |
| FIDAP | • | • | | | • | | |
| FLASH2 | • | | | | • | | |
| HIFINEL | • | | | | | | • |
| LAWPILE | • | | | | | | |
| LISA | • | • | • | • | | | |
| LUSAS | • | • | | • | • | • | • |
| MARC | • | • | • | • | • | • | • |
| MBB-MAN-ICES-STRUDL | • | • | • | • | | • | • |
| MICAS | • | | | | | | |
| MIX | • | | | • | • | | |
| MODEL | • | | | | | • | • |
| MODULEF | • | • | • | | | | • |
| MSC/NASTRAN | • | • | • | • | • | | • |
| PAFEC | • | • | • | • | | • | • |
| PDA/PATRAN-G | • | • | | | | | |
| PECET | • | | | | | | |
| PREFEM & SERFEM | • | | | | | | |
| RAFTS | • | | | | | | |
| SCIA | • | • | • | | | | • |
| SESAM-69 | • | • | • | | • | • | • |
| SET | • | | | | | | • |
| STARS | • | • | • | • | | | |
| STATIK | • | | | | | | |
| STYDYNL | • | • | • | • | • | | |
| THAFEM | | | | | | | • |
| TITUS | • | • | • | • | • | • | • |

*Figure 21: Summary of the capabilities of finite element and boundary element computer codes for stress analysis (Brebbia, 1985).*

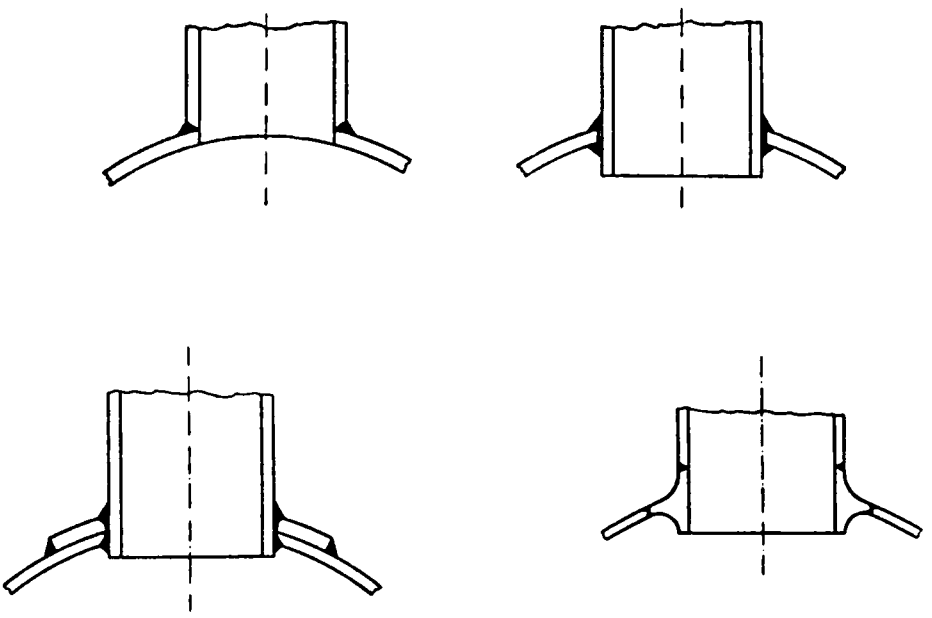

*Figure 22: Typical types of shell branches.*

### *5.8.1 Holes in Plates and Cylindrical Shells*

Analytical solutions are available for the stress concentrations around holes in flat plates under tension or bending, and also for simple cylindrical shells under external pressure loading. Peterson (1974) lists a variety of analytical and experimental results in graphical form. Consider first the case of an elliptical hole in a thin, flat plate of infinite extent. The classic solution obtained by Inglis is described in some detail by Durelli (1981).

The uniform stresses $\sigma_z$ and $\sigma_y$ are applied to an infinite sheet containing an elliptical hole with semi-axes a and b as shown in Figure 23(a). The stresses at the edge of the hole obtained by Inglis are

$$\sigma_\alpha = \tau = 0$$

$$\sigma_\beta = \frac{(\sigma_z + \sigma_y)\sinh(2\alpha_o) + (\sigma_z - \sigma_y)[\cos(2\phi) - \exp(2\alpha_o)\cos 2(\phi - \beta)]}{\cosh(2\alpha_o) - \cos(2\beta)} \qquad (63)$$

where $\alpha$ and $\beta$ are elliptical coordinates such that $\alpha = \alpha_o$ is constant at the edge of the hole so $\sigma_\alpha$ represents the stress perpendicular to the edge of the hole and $\sigma_\beta$ the stress tangent to the hole. At the ends of the major axis (for $\phi = 0$) z = a, y = 0, $\beta = 0$ and the tangential stress is

$$\sigma_\beta = \sigma_y (1 + 2a/b) - \sigma_z \tag{64}$$

At the ends of the minor axis ($\phi = 0$)

$$\sigma_\beta = \sigma_z (1 + 2b/a) - \sigma_y \tag{65}$$

For the uniaxial stress case ($\sigma_z = 0$) the stress concentration factor at the end of the major axis is

$$K_t = 1 + 2\sqrt{a/\rho} \tag{66}$$

where $\rho = b^2/a$ is the radius of curvature at the end of the major axis.

In the case of cylindrical bending (as opposed to biaxial loading above) with the geometry shown in Figure 23(b), Savin (1961) provides the following solution. The moments at the edge of the hole are

$$M_r = 0$$
$$M_\gamma = M\,[1 + 2(1 + \nu)(1 - m)(m - \cos 2\gamma) / (3 + \nu)(m^2 - 2m \cos 2\gamma + 1)] \tag{67}$$

where r and $\gamma$ are polar coordinates and m = (a-b)/(a+b). The maximum moment occurs at $\gamma = \pm \pi/2$ and the minimum at $\gamma = 0, \pi$. The stress corresponding to the moment is

$$\sigma = 12\rho\, M_\gamma / h^3 \tag{68}$$

where $\rho$ is the distance from the midplane of the plate in the thickness direction.

The stress concentration factor for a circular hole in a cylindrical shell is higher than for a hole in a flat plate. The Luré solution described in Savin's (1961) compendium is applicable to a hole in a capped, simple cylindrical shell subjected to pressure p, provided the radius of the hole r is small relative to the shell radius R and thickness h

$$r^2 << Rh \tag{69}$$

The hole is subjected to uniform biaxial stress $\sigma_z = pR/2h$ and $\sigma_\gamma = pR/h$ as described in Section 3. The tangential stress at the edge of the hole is

$$\sigma_\gamma = (pR/h)\,\{3/2 + \cos(2\gamma) + \pi r^2 \sqrt{3(1 - \nu^2)}\,[4 + 5\cos(2\gamma)] / 8Rh\} \tag{70}$$

where $\gamma$ is the polar angular coordinate (Figure 23b). The maximum stress occurs at $\gamma = 0$. The stress concentration factor is

$$K_t = 5/2 + 9\pi r^2 \sqrt{3(1 - \nu^2)} / 8Rh \tag{71}$$

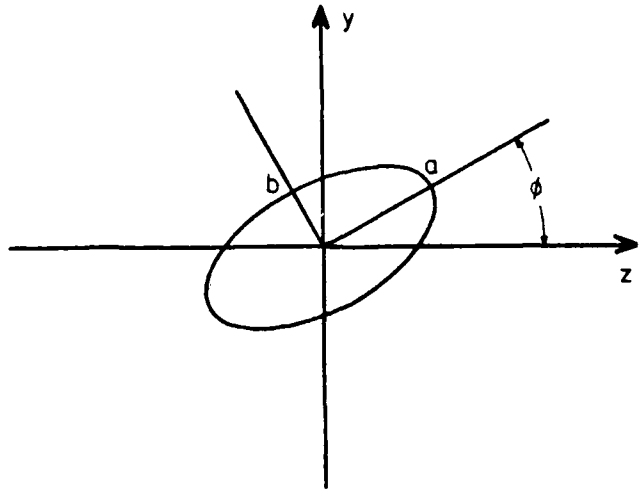


a.

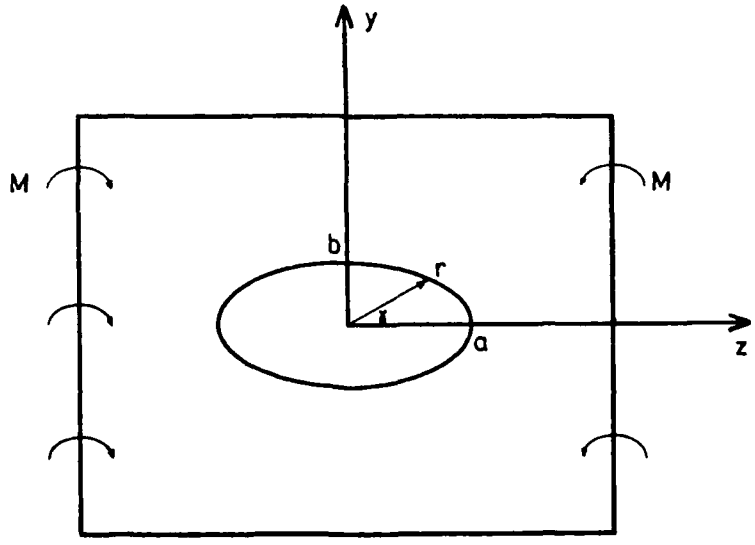


b.

*Figure 23: Geometries of elliptical holes discussed in Section 5.8.1.*

compared with 5/2 for a circular hole in a flat plate. For the particular case R = 3 m, h = 25 mm, r = 250 mm and $\nu = 0.3$, the SCF is 7.4 (this barely satisfies the condition $r^2 << Rh$). For r = 50 mm the SCF is 2.7.

Eringen et al. (1965) criticize the Luré solution on the grounds of inappropriate boundary conditions. They present results in graphical form for a thin, circular cylindrical, elastic shell with a circular hole, subjected to various loadings. The effect of pressure acting as a shear loading on the edge of the hole is taken into account.

In the case of a submarine pressure hull, the stress around hull penetrations is reduced by the addition of stiffening pads. The hull stiffening rings also reduce the circumferential stress to below pR/h (also introduce bending moments) but are not expected to have a large effect on the stress concentration factor.

### *5.8.2 Local Loads Applied to Cylindrical Shells*

Local loads have generally been considered in the form of line loads, area loads, or loads applied via nozzles or other local attachments. Summaries are given by Kitching (1970) and Kraus (1967) for the case of local loading of cylindrical shells. Only geometrically simple cases are amenable to analytical calculations.

Hoff and co-workers (Hoff, 1954; Hoff et al. 1954) obtained analytical results for moments and radial loads applied along axial lines or circumferential arcs. Expressions for the shell deflections u, v and w are obtained (containing eight arbitrary constants) which automatically satisfy the Donnell cylindrical shell equations. The expressions have the form

$$w = \cos(nz/R)\{\exp(-\alpha_1\theta)\,[A_1\cos(\beta_1\theta) + A_2\sin(\beta_1\theta)] + \exp(-\alpha_2\theta)[A_3\cos(\beta_2\theta) + A_4\sin(\beta_2\theta)]$$
$$+ \exp(\alpha_1\theta)[A_5\cos(\beta_1\theta) + A_6\sin(\beta_1\theta)] + \exp(\alpha_2\theta)[A_7\cos(\beta_2\theta) + A_8\sin(\beta_2\theta)]\} \quad (72)$$

Since the deflection must decay with distance from the line load, only the negative exponentials are retained. The four remaining constants $A_1$ to $A_4$ are determined by the boundary conditions. The stresses and stress resultants are readily calculated once the deflections are found. Different types of line load distributions can be handled using Fourier series methods. The approach is analogous to that used to obtain edge loading solutions in Section 5.6.

Kitching also aummarizes the analysis of loads applied over rectangular areas of a cylindrical shell. This can be done by direct integration of the effects of line loads, or can be done more directly using Bijlaard's (1955a) procedure (see also Bijlaard, 1954, 1955b, 1959a). The British Standard BS 1515 : Pt 1 : 1965 (as amended) Appendix A contains numerous graphs allowing calculation of stresses in cylindrical and spherical shells adjacent to moments and radial loads applied to rectangular areas, axial lines and circumferential arcs. Some other relevant documents are Findlay and Timmins (1987) which gives a brief review of the development of the field, British Standard BS 5500 Appendix G, and Bedri et al. (1983). Tooth and Motashar (1989) consider the case of radial loading via a rigid rectangular attachment rather than the usual uniformly distributed loading. This method of loading causes stress concentration at the edges of the attachment.

The third major class of local loadings which have been studied consists of loadings applied over more circular areas of the cylinder surface. This type of loading is important in

the case of intersecting cylinders (such as pressure vessel nozzles, or hatches in submarine hulls). There is a large volume of literature. Graphical results for various types of loading applicable to cylindrical nozzles in cylindrical pressure vessels are presented by Mershon et al. (1984). Gill et al. (1970) give a brief overview of the theory for branches in spherical and cylindrical pressure vessels. Teixeira et al. (1981) present a simplified method for calculating stresses due to loadings on branches in cylindrical vessels. Decock (1973) and Spence and Carlson (1967) consider fatigue assessment. Leckie and Penny (1963) and Bijlaard (1959b) consider branches in spherical vessels.

Superposition of stresses due to external pressure and those due to branches is not conservative (it is for internal pressure). This difficulty can be overcome using an approximate method described by Bijlaard (1955a).

## *5.9 Residual Stresses*

The majority of fatigue and toughness problems associated with high strength steel submarine hulls are limited to welds and associated heat affected zones (Roberts and Smith, 1988). The driving force for fatigue in these locations is the distribution of tensile residual/restraint stresses caused by welding (Kilpatrick, 1986) and the stress concentrating effect of the weld profile itself. Without these stresses, the cyclic compressive stresses due to hydrostatic loading would be largely non-damaging. Another significant source of residual stress is the process of cold rolling the hull plate and stiffening rings to the required curvature. These sources are considered in Sections 5.9.1 and 5.9.2 respectively.

In addition to the fatigue problem, residual stresses are important from the point of view of shell buckling. A brief review is given by Bushnell (1985, p. 192). Kendrick (1985) points out that residual stresses can have a large effect on collapse pressure if initial shape imperfections are small, but have a lesser effect when the shape imperfections are greater (i.e. the two effects are not additive).

It is a relatively simple matter to calculate the residual stresses due to cold bending of plate. Calculation of welding stresses is more difficult, but has been attempted for simple geometries using a variety of numerical modelling techniques (see for example Masubuchi, 1980; Jones et al., 1977; Bushnell, 1985). Only a simple analysis applicable to the fatigue problem is attempted here.

### *5.9.1 Residual Stresses due to Cold Bending of Plates*

Consider the simple case of an elastic-perfectly plastic plate which is initially bent to radius of curvature $R_o$ and then springs back to radius R. Assuming linear strain distribution through the thickness, the strain and stress when bent to radius $R_o$ are

$$\epsilon_\theta = \rho/R_o \tag{73}$$

$$\sigma_\theta = \begin{cases} E\rho/R_o & \text{for } \rho \le \sigma_y R_o / E \\ \sigma_y & \text{for } \rho \ge \sigma_y R_o / E \end{cases} \tag{74}$$

where $\rho$ is the distance from the mid-plane of the plate, $\sigma_y$ is its yield stress and E its Young's modulus.

Ignoring Bauschinger effect and assuming elastic springback, the corresponding quantities when the plate returns to radius R are

$$\epsilon_\theta = \rho / R \tag{75}$$

$$\sigma_\theta = \begin{cases} E\rho/R & \text{for } \rho \le \sigma_y R_o / E \\ \sigma_y - E\rho\,(1/R_o - 1/R) & \text{for } \rho \ge \sigma_y R_o / E \end{cases} \tag{76}$$

Equation (76) describes the residual stress distribution. It has a characteristic zig-zag shape as shown in Figure 24.

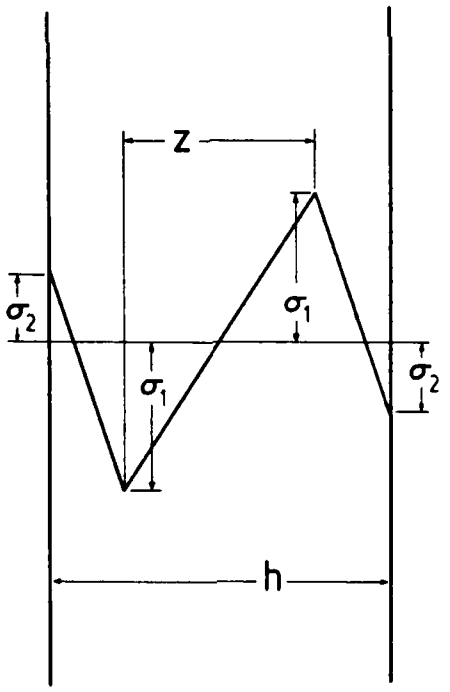


*Figure 24: Characteristic residual stress distribution through the thickness h of an elastic-plastic plate after cold bending to a curved shape.*

The radius of curvature $R_o$ which must be applied to the plate in order to achieve final radius R can be found from the condition that the bending moment must be zero in the final state

$$M = 0 = 2 \int_0^{\sigma_y R_o/E} E\rho^2/R \, d\rho \qquad (77)$$

$$+ 2 \int_{\sigma_y R/E}^{h/2} \sigma_y \rho - E\rho^2 (1/R_o - 1/R) \, d\rho$$

where h is the plate thickness. After a little algebra we obtain

$$R_o = R (4 - 3Q^2 + Q^3) / Q^3 \qquad (78)$$

where Q is the parameter $Eh/\sigma_y R_o$. The quantities defining the zig-zag residual stress distribution (Figure 24) are

$$\sigma_1/\sigma_y = R_o/R = (4 - 3Q^2 + Q^3) / Q^3 \qquad (79)$$

$$\sigma_2/\sigma_y = (4 - Q^2) / 2Q^2 \qquad (80)$$

$$z/h = 2/Q \qquad (81)$$

Kendrick (1970) shows values of these three quantities plotted against the parameter

$$F = Eh/\sigma_y R = R_o Q/R = (4 - 3Q^2 + Q^3) / Q^2 \qquad (82)$$

This is reproduced as Figure 25. In the case of submarine hulls, F has a typical value of 3, and the circumferential residual stress peaks due to cold bending are about half the yield stress. The outer surface is in compression and the inner surface in tension.

More sophisticated calculations of the residual stress distribution have been made by incorporating various work hardening rules in place of the simple elastic-perfectly plastic model considered above (e.g. Shama, 1970). However, the elastic-plastic model is quite good for submarine hull steels, and larger error is likely to accrue from lack of precise knowledge of the yield strength of the particular plate than from neglect of work hardening (or the Bauschinger effect).

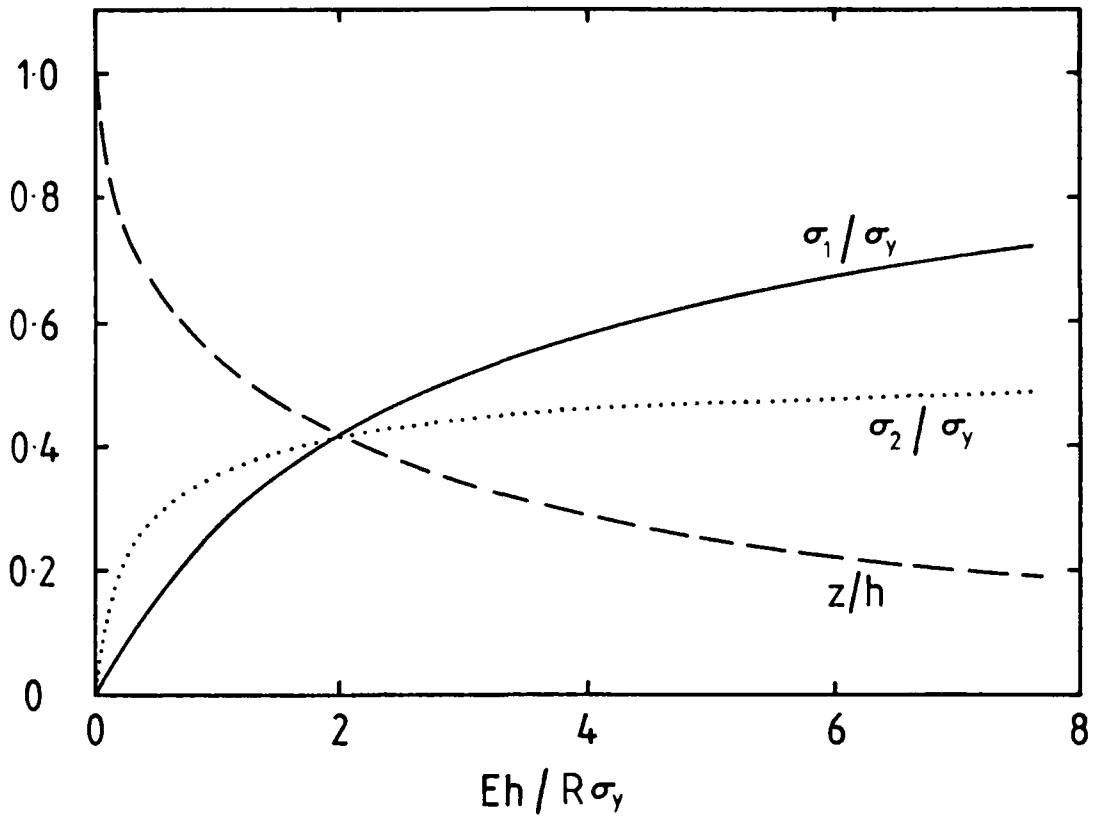


*Figure 25: Effect of the dimensionless parameter $Eh/R\sigma_y$ on the three parameters defining the residual stress distribution (Figure 24) of a plate after cold bending to a curved shape.*

### *5.9.2 Residual Stresses due to Welding*

Welding residual stresses arise primarily from the shrinkage of the weld metal and HAZ on cooling from high temperature. The resulting stress levels depend heavily on the restraint imposed on this shrinkage by the remainder of the structure. For high strength steels typical of those used to construct submarine hulls, a temperature change of 200-300 K is sufficient for the shrinkage stress to reach the yield stress if thermal movement is fully restrained. The residual stress has short range and long range components due to non-uniform plastic strains near the weld and external restraint respectively (Lidbury, 1984). The short range stresses can be considered to be confined to distances within a few plate thicknesses of the weld. Heavy section weldments are normally expected to have residual stress close to the yield stress in the longitudinal direction throughout the fusion zone, and for a significant portion of the joint thickness in the transverse direction. The residual stress in the through thickness direction is much lower due to lack of restraint.

Short range residual stresses are difficult to treat analytically. However, the long range restraint stresses are more tractable. In the case of submarine hulls, circumferential seam and tee-butt welds have received the most attention.

Faulkner (1977) considers two main weld shrinkage actions in the tee butt welds between the stiffening rings and hull plate illustrated in Figure 26:

(i) Longitudinal (along the weld) shrinkage giving rise to a region of residual stress of tensile yield stress magnitude in the circumferential direction. This region comprises a width 2 $\eta h$ of the plating and depth $\eta h$ (or 0.75 $\eta h$ according to Smith and Kirkwood, 1977) of the stiffener web adjacent to the weld. The parameter $\eta$ varies in magnitude depending on the welding conditions, and the yield stress and thickness of the members joined. Faulkner quotes a value of 1.5 for a ring stiffened structure. Smith and Kirkwood quote 2-4 for small cylinders with frames attached by continuous, single-pass welds, and $\eta << 2$ for submarine hulls and multi-pass welds. The tensile residual stress near the weld is balanced by an approximately uniform compressive stress $\sigma^p_{\theta 1}$ (in the circumferential direction) distributed over the remainder of the cross section.

(ii) Transverse (across the weld) shrinkage applies a longitudinal bending moment to the plating and causes concertina-like distortion. The additional circumferential stress $\sigma^p_{\theta 2}$ in the shell is balanced by stress $\sigma^f_\theta$ in the ring stiffener.

Although the longitudinal shrinkage would cause reduced shell diameter at the ring stiffener locations, the bending moment caused by the transverse shrinkage acts in the opposite direction. The net effect is that the rings stand out (for internal framing) as shown in Figure 26. The shell bends inwards between the rings to form the concertina distortion observed in practice.

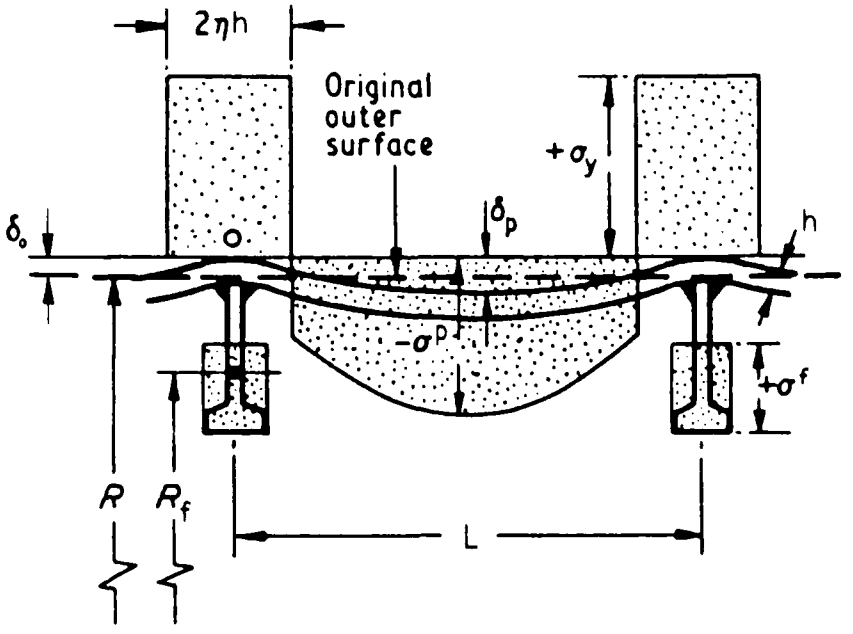


*Figure 26: Residual stresses and distortions of a ring stiffened cylinder due to circumferential tee butt welds (from Faulkner, 1977).*

The circumferential stress $\sigma^p_{\theta 1}$ necessary to balance the yield tension block due to longitudinal weld shrinkage is easily calculated as

$$\sigma^p_{\theta 1} = - 2\eta h \sigma_y / (L - 2\eta h) \tag{83}$$

where L is the spacing between ring stiffeners and h is the plate thickness.

Turning to the transverse shrinkage, practical experience with submarines and offshore structures (Faulkner, 1977) indicates that the amplitude of the concertina distortion is typically

$$\delta_p = h / 10 \tag{84}$$

Assuming a sinusoidal distortion pattern

$$\delta = \delta_o - \delta_p \sin (\pi z/L) \tag{85}$$

where z is taken to be zero at the location of the stiffening ring and $\delta_o$ is yet to be found (see Figure 26), the induced circumferential stresses in the plate and in the frame are respectively

$$\sigma^p_{\theta 2} = E\delta / R \tag{86}$$

$$\sigma^f_{\theta} = E\delta_o / R_f \tag{87}$$

At equilibrium the loads in the stiffener and plating must balance each other, allowing $\delta_o$ to be determined as follows

$$O = E\delta_o A_f / R_f + 2 \int_0^{L/2} Eh [\delta_o - \delta_p \sin (\pi z/L)] / R \, dz$$

$$\delta_o = 2\delta_p / \pi (1 + A_f R/R_f hL) \tag{88}$$

The circumferential stresses in the plate and frame due to both longitudinal and transverse weld shrinkage are therefore

$$\sigma^p_{\theta} = \begin{cases} \sigma_y & \text{for } O < z < \eta h \\ -2\eta h\sigma_y / (L-2\eta h) + (Eh/10R)[2/\pi (1 + A/hL) - \sin(\pi z/L)] & \text{for } \eta h < z < L/2 \end{cases} \tag{89}$$

$$\sigma^f_{\theta} = Eh / 5\pi R_f (1 + A/hL) \tag{90}$$

where A is the modified frame area $A_f R/R_f$. This result reproduces the expressions given by Faulkner. For an internally stiffened cylinder, the stiffener is in tension and the plating is in tension near the frame and in compression near mid-bay as a result of the across-the-weld shrinkage. The peak compressive stress in the plating is of the order of $\sigma_y/5$ (as measured on a submarine hull during construction). This occurs at mid-bay.

Faulkner's analysis is concerned mainly with the collapse strength of ring stiffened cylinders. From the fatigue viewpoint, the longitudinal stresses acting across the weld are more significant because cracking is most likely to initiate at weld bead toes. The bending moment (and hence stresses) can be calculated from the curvature of the plating.

The distortions arising from welding and other effects such as misaligments are important not only because of the accompanying residual stresses. These shape imperfections also modify the response of the structure to externally applied loadings such as hydrostatic pressure. Buckling pressure can be greatly reduced by the presence of shape imperfections.

## *5.10 Shape Imperfections*

Shape imperfections can be broadly classified into two groups: diffuse imperfections such as out-of-roundness and concertina distortion, and localised imperfections such as misfit or misalignment between adjacent welded plates or hull sub-units. The latter group are better described as stress concentrations and are considered in Section 5.11. Generally speaking, both groups of shape imperfection introduce additional bending stresses which would not be present in a geometrically perfect cylindrical or spherical shell.

It is usual to consider the diffuse shape imperfections as having two components. The variation in shape in the circumferential direction is known as out-of-roundness. The variation in shape in the longitudinal direction of a cylindrical shell is known as the axisymmetric shape imperfection (an example being concertina distortion due to the welded joints between hull plating and ring stiffeners). Both have been examined in some detail because of the strong influence they can have on the collapse pressure.

Out-of-roundness shape imperfections reduce collapse pressure in the same way that eccentric loading of a column reduces its buckling load (Wenk, 1961; Kendrick, 1985). The degree of strength reduction depends on the amplitude and wavelength of the imperfection, and also on the level of residual stresses. Imperfections are particularly damaging if they match one of the buckling modes of the cylinder. Tolerances on out-of-roundness are therefore restricted to half the plate thickness or less (Wenk, 1961).

The concertina distortion due to welding has already been considered in Section 5.9.2. The initial distortion, combined with the axial load due to pressure on the end closures of a cylindrical shell, again acts to introduce additional bending stresses as for an imperfect or eccentrically loaded column. In the case of internal stiffening rings, collapse pressure is reduced compared with the case of external rings, where the initial distortion is outwards between the rings (in the opposite direction to the displacement under pressure loading).

Fourier series methods are the usual approach to calculating the additional stresses due to shape imperfections. The initial imperfection can be expressed in the form (Kendrick, 1964):

$$w_o = \sum_{m=1}^{\infty} \sum_{n=1}^{\infty} C_{mn} \cos(n\theta) \sin(m\pi z/L) \qquad (91)$$

The deflections and stresses in the shell due to hydrostatic pressure can then be calculated. The results consist of a term representing the behaviour of a perfect shell, and an additional term due to the imperfection. Wilson (1956b) obtained results in a similar form considering just the axisymmetric concertina distortion. Before calculations of this type can be carried out, it is necessary to know the actual form of the shape imperfections.

## *5.11 Stress Concentrations*

Almost all of the discussion in previous sections has been concerned with stress analysis within the framework of thin shell theory. Some of the basic assumptions of this theory are that the thickness of the shell is small relative to the radius of curvature, and that stresses and strains in the through thickness direction are small enough to be ignored. While the theory works well in describing the general behaviour of a structure, it does not allow accurate calculation of stresses at small scale structural details where the geometry changes rapidly on the length scale given by the thickness of the shell. However it is at just such structural details that fatigue cracking is likely to initiate because of stress concentration effects (e.g. changes of plating thickness, welds). These higher order stress concentration factors can be calculated if not too high (< 10) using a general finite element analysis program to model the structural detail. A shell theory calculation is used to obtain the forces and moments acting on the detail at a distance of several shell thicknesses away from the detail (Kendrick, 1970).

The numerical approach to calculating higher order stress concentrations is beyond the scope of this review. However, a large body of information on stress concentrations has been developed by calculation, numerical methods and experimental methods. Compilations such as Peterson (1974) provide easy access to much of this information. Some relevant cases considered by Peterson are:

(i) Weld profiles (pages 94, 95)
(ii) Change of thickness of cylindrical pressure vessel wall (page 97)
(iii) Holes of various geometries in plate under a biaxial stress state (Chapter 4)
(iv) Reinforced holes (Chapter 4)

Additional results for stress concentration factors at various types of weld are given by Gurney (1975, 1979a, 1979b).

It is notoriously difficult to predict fatigue behaviour theoretically, because of the difficulty of analysing stresses/strains at structural details. (Further difficulties arise in obtaining reliable load histories, and in taking into account load sequence effects and environmental interactions). The experimental approach is still widely used. Research on offshore tubular structures has generated a large amount of information available in the open literature. Results for submarine hulls are more restricted. One of the difficulties with the experimental approach is that models must be of large scale in order to reproduce realistic welding residual/restraint stresses.

# 6. *Fatigue*

Most of the information available on the fatigue of submarine hulls derives from the UK fatigue program carried out at ARE, Dunfermline (e.g. Kilpatrick, 1986). As a submarine hull is subjected to fluctuating compressive stresses, fatigue problems would not initially be expected. However, when the compressive applied stresses are superimposed on tensile residual welding stresses, at least part of the cycle is tensile and therefore damaging from a fatigue viewpoint.

The ARE program includes the measurement and calculation of residual and applied stresses in scale models tested to failure in fatigue chambers (large pressure vessels allowing pressure cycles to be applied to the models). The work appears to concentrate on the stiffener-hull tee butt welds. Allowable fatigue design stresses are lowest at such axisymmetric stress concentrations. Higher stresses are allowed at point stress concentrations such as hull penetrations. Models tested to date failed by circumferential cracking through the hull plate, initiating at the toes of stiffener tee butt welds as shown schematically in Figure 27. Bending stresses after welding were typically 80% of the material yield stress at the weld toes, however a complicating feature of this type of work is that the residual stress distribution is modified during the first few load cycles (shakedown) due to plastic yielding in compression.

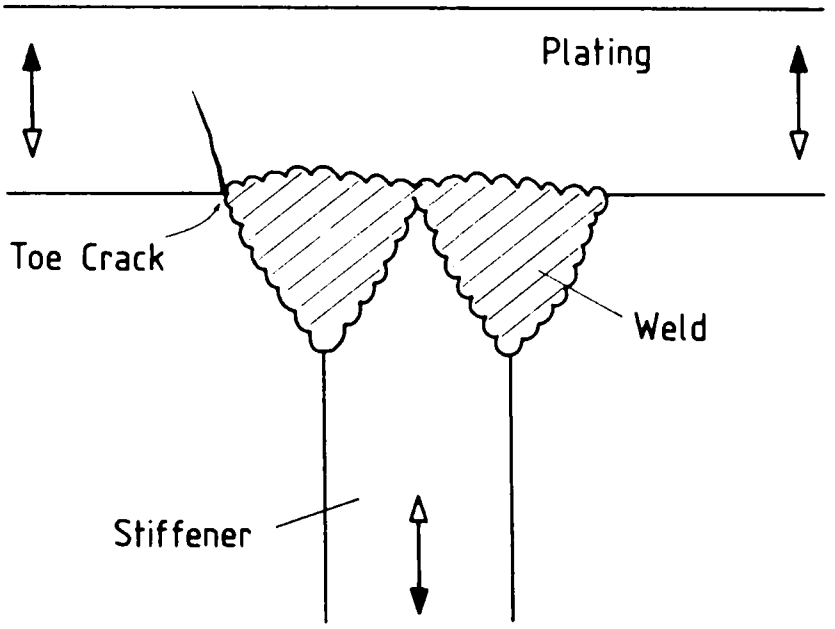


*Figure 27: Fatigue crack propagation path in ARE scale model fatigue tests (from Kilpatrick, 1986).*

Fatigue of welded structures in general is reviewed in great detail by Gurney (1979a). The following discussion is largely derived from that work. Consider a residual stress distribution and a superimposed cyclic applied stress distribution. If the yield stress is not reached, then the total stress is simply the sum of the two components. If the yield stress is reached then plastic deformation occurs, and that part of the structure is subsequently subjected to a stress cycle which ranges from the yield stress downwards, regardless of the stress ratio of the applied stress. In many cases the residual stresses alone are of yield stress magnitude so this condition is quite common.

As an example, consider a tensile residual stress of yield stress magnitude ($\sigma_r = \sigma_y$) with a cyclic applied stress ranging from $-\sigma_2$ to $+\sigma_1$. The stress range is $(\sigma_1 + \sigma_2)$ and the total stress varies between $\sigma_y$ and $\sigma_y - (\sigma_1 + \sigma_2)$. The fatigue behaviour is dependent only on the stress range and is independent of (applied) mean stress. Compressive applied stresses are just as damaging as tensile stresses.[2]

Ignoring residual stress redistribution, and considering the zero-compression loading applicable to a submarine hull ($\sigma_1$ in the discussion above), the total stress ranges from $\sigma_r$ down to $\sigma_r - \sigma_2$. If $\sigma_2$ is less than $\sigma_r$ then the stress remains tensile throughout the cycle. If $\sigma_2$ is greater than $\sigma_r$ then the total stress is compressive for part of the cycle, the damaging part of the cycle is the stress range $\sigma_r$ to zero, and fatigue life should be independent of $\sigma_2$ (unless $\sigma_2$ is sufficiently large to cause yielding in compression). It is clear that the fatigue assessment of a submarine hull design must encompass both tensile residual stresses and the (usually compressive) applied stresses.

# *7. Conclusion*

Analytical solutions are available for a large number of shell structures with relatively simple geometries (usually axisymmetric) typical of those found in submarines and other pressure vessels. They give a good picture of the general stress distribution due to geometrically simple load distributions such as hydrostatic pressure. However, analytic solutions are not adequate for obtaining stresses at many structural details where fatigue cracking is likely to initiate. For these details the analytical methods must be augmented by experimental methods or numerical computer calculations. A further difficulty in predicting fatigue behaviour is the accurate calculation or measurement of residual stresses built into the structure during fabrication. Future work should address these questions.

2 One exception to this statement is when yielding in one area occurs in compression, resulting in the reduction of the balancing residual tensile stress in an adjacent area. Fatigue crack tip plasticity also modifies the local residual stress distribution.

# 8. References


Almroth, B.O., Brogan, F.A. and Stanley, G.M. (1980). *Structural analysis of general* shells; user instructions for STAGSC-1. California: Lockheed Palo Alto Research Laboratory.

Atkins Research and Development Ltd (1982). *ASAS/NL user manual.* Surrey: Epsom)

Baker, E.H., Kovalevsky, L. and Rish, F.L. (1972). *Structural analysis of shells.* New York: McGraw Hill.

Bedri, R., McLeish, R.D. and Gill, S.S. (1983). Some observations on the calculation of stresses due to local loads on cylindrical shells using BS 5500 : Appendix G. *International Journal of Pressure Vessels and Piping*, **13**, 227-251.

Bijlaard, P.P. (1954). Stresses from radial loads and external moments in cylindrical pressure vessels. *Welding Journal Research Supplement*, **33** (12), 615-623s.

Brebbia, C.A. (1985). *Finite element systems - a handbook*, 3rd edn. Berlin: Springer-Verlag.

Bushnell, D. (1974). Stress stability and vibration of complex, branched shells of revolution. *Computers and Structures*, **4**, 399-435.

Bushnell, D. (1985). *Computerized buckling analysis of shells.* Dordrecht: Martinus Nijhoff.

Bijlaard, P.P. (1955a). Stress from local loadings in cylindrical pressure vessels. *Journal of Applied Mechanics*, **77** (6), 805.

Bijlaard, P.P. (1955b). Stresses from radial loads and external moments in cylindrical pressure vessels. *Welding Journal Research Supplement*, **34** (12), 608-617s.

Bijlaard, P.P. (1959a). Additional data on stresses in cylindrical shells under local loading. *Welding Research Council Bulletin* # 50.

Bijlaard, P.P. (1959b). Stresses in a spherical vessel from radial loads acting on a pipe. Stresses in a spherical vessel from external moments acting on a pipe. Influence of a reinforcing pad on the stresses in a spherical vessel under local loading. *Welding Research Council Bulletin* # 49.

Cloud, R.L. (1970). Pressure vessel ends. In, S.S. Gill (ed.) *The stress analysis of pressure vessels and pressure vessel components*, pp. 167-218. Oxford: Pergamon.

Compton-Hall, R. (1989). The incredible shrinking submarine. *New Scientist*, 1 April 1989.

Decock, J. (1973). Determination of stress concentration factors and fatigue assessment of flush and extruded nozzles in welded pressure vessels. In *2nd International Conference on Pressure Vessel Technology*, p. 821-834.

de Hart, R.C. (1969). External pressure structures. In, J.J. Myers, C.H. Holm and R.F. McAllister (eds.) *Handbook of ocean and underwater engineering*. New York: McGraw-Hill.

Durelli, A.J. (1981). Stress concentrations. In, G.C. Sih (ed.) *Experimental evaluation of stress concentration and intensity factors*. The Hague: Martinus Nijhoff.

Eringen, A.C., Naghdi, A.K. and Thiel, C.C. (1965). State of stress in a circular cylindrical shell with a circular hole. *WRC Bulletin* # 102.

Faulkner, D. (1977). Effects of residual stresses on the ductile strength of plane welded grillages and of ring stiffened cylinders. *Journal of Strain Analysis*, **12** (2), 130-139.

Findlay, G.E. and Timmins, W. (1987). Local radial loads on cylinders : BS 5500 Predictions v Experimental results. *International Journal of Pressure Vessels and Piping*, **27** (1), 33-48.

Flügge, W. (1960). *Stresses in shells*. Berlin: Springer-Verlag.

Friedman, N. (1984). *Submarine design and development*. Annapolis, Maryland: Naval Institute Press.

Gibson, J.E. (1980). *Thin shells - computing and theory*. Oxford: Pergamon.

Gill, S.S. (1970). Basic principles. In, S.S. Gill (ed.) *The stress analysis of pressure vessels and PV components*, pp. 7-71. Oxford: Pergamon.

Gill, S.S., Leckie, F.A. and Penny, R.K. (1970). Pressure vessel branches. ibid pp. 73-116.

Gurney, T.R. (1975). *Finite element analyses of some joints with the welds transverse to the direction of stress* (Research Report E/62/75). Cambridge: The Welding Institute.

Gurney, T.R. (1979a). *Fatigue of welded structures*, 2nd edn. Cambridge: Cambridge University Press.

Gurney, T.R. (1979b). *Stress intensity factors for cracks at the toes of transverse butt welds* (Research Report 88/1979). Cambridge: The Welding Institute.

Hampe, E. (1964). *Statik rotationssymmetrischer flächentragwerke*. Berlin: VEB Verlag für Bauwesen.

Harvey, J.F. (1985). *Theory and design of pressure vessels*. New York: Van Nostrand Reinhold.

Hoff, N.J. (1954). Boundary valve problems of the thin-walled circular cylinder. *Journal of Applied Mechanics*, **21**, 343-350.

Hoff, N.J., Kempner, J. and Pohle, F.V. (1954). Line load applied along generators of thin-walled circular cylindrical shells of finite length. *Quarterly of Applied Mathematics*, **11**, 411-426.

Jane's (1989). Italy's small submarine aimed at export market. *Jane's Defence Weekly*, 25 March 1989, p. 505.

Jones, R.F., Armen, H. and Fong, J.T. (1977). Numerical modeling of manufacturing processes. *Winter Annual Meeting of ASME.*

Kendrick, S. (1964). *Structural design of submarine pressure vessels (U)* (Report NCRE-R483) (Unclassified report). Dunfermline, Fife: Naval Construction Research Establishment.

Kendrick, S. (1970). Externally pressurized vessels. In, S.S. Gill (ed.) *The stress analysis of pressure vessels and PV components*, pp. 405-507. Oxford: Pergamon.

Kendrick, S. (1985). Ring-stiffened cylinders under external pressure. In, R. Narayanan (ed.) *Shell structures - stability and strength*, pp. 57-95. London: Elsevier Applied Science.

Kilpatrick, I.M. (1986). The fatigue characteristics of submarine structures subjected to external pressure cycling. In *Advances in marine structures*, ARE, Dunfermline, May 1986. London: Elsevier Applied Science.

Kitching, R. (1970). Local loading and local attachments. In, S.S. Gill (ed.) *The stress analysis of pressure vessels and PV components*, pp. 221-265. Oxford: Pergamon.

Kraus, H. (1967). *Thin elastic shells.* New York: Wiley.

Krenzke, M.A. and Short, R.D. (1959). *Graphical method for determining maximum stresses in ring-stiffened cylinders under external hydrostatic pressure* (Report DTMB-R1348). David Taylor Model Basin.

Leckie, F.A. and Penny, R.K. (1963). Stress concentration factors for the stresses at nozzle intersections in pressure vessels. *WRC Bulletin* # 90.

Lidbury, D.P.G. (1984). The significance of residual stresses in relation to the integrity of LWR pressure vessels. *International Journal of Pressure Vessels and Piping*, **17** (4), 197-328.

Masubuchi, K. (1980). *Analysis of welded structures.* Oxford: Pergamon.

Moshaiov, A. and Joelson, E.R. (1989). Theory and application of a bi-metal ring stiffened cylinder under external pressure. *Journal of Ship Research*, **33** (4), 291-297.

Mershon, J.L., Mokhtarian, K., Ranjan, G.V. and Rodabaugh, E.C. (1984). Local stresses in cylindrical shells due to external loadings on nozzles. *WRC Bulletin* 297.

Novozhilov, V.V. (1959). *The theory of shells*. Groningen: Noordhoff.

Peterson, R.E. (1974). *Stress concentration factors*. New York: Wiley.

Popov, E.P. (1978). *Mechanics of materials*, 2nd ed. Englewood Cliffs, NJ: Prentice-Hall.

Roberts, M.L. and Smith, C.S. (1988). Design of submarine structures. In, *1988 Undersea Defence Technology Conference*, London, Oct. 26-28, 1988, pp. 217-225. Tunbridge Wells: Microwave Exhibitions and Publishers.

Salerno, V.L. and Pulos, J.G. (1951). *Stress distribution in a circular cylindrical shell under hydrostatic pressure supported by equally spaced circular ring frames* (Report 171-A). Brooklyn: Poly. Inst.

Savin, G.N. (1961). *Concentration of stress around holes* (Translation). Oxford: Pergamon.

Shama, M.A. (1970). Cold forming residual stresses and their effect on the accuracy of post-forming operations. *European Shipbuilding*, **2**, 23-26.

Short, R.D. and Bart, R. (1959). *Analysis for determining stresses in stiffened cylindrical shells near structural discontinuities* (Report DTMB-R1065). David Taylor Model Basin.

Smith, C.S. and Kirkwood, W. (1977). Influence of initial deformations and residual stresses on inelastic flexural buckling of stiffened plates and shells. In, P.J. Dowling, J.E. Harding and P.A. Frieze (eds.), *Steel plated structures*, pp. 838-863. London: Crosby Lockwood Staples.

Sokolnikoff, I.S. (1956). *Mathematical theory of elasticity*, 2nd ed. New York: McGraw-Hill.

Spence, J. and Carlson, W.B. (1967). A study of nozzles in pressure vessels under pressure fatigue loading. *Proceedings of the Institute of Mechanical Engineers*, **182** (31), 657-684.

Stout, R.D. and Pense, A.W. (1965). Effect of composition and microstructure on the low cycle fatigue strength of structural steels. *Transactions of the ASME Journal of Basic Engineering*, **87** (2), 269-274.

Teixeira, M.A., McLeish, R.D. and Gill, S.S. (1981). A simplified approach to calculating stresses due to radial loads and moments applied to branches in cylindrical pressure vessels. *Journal of Strain Analysis*, **16** (4), 217-226.

Thompson, A.D.E. and Christopher, P.R. (1973). How materials properties affect the design of submersible structures. In, *The Relevance of Fracture Toughness to the Design and Reliability of Military Equipment (Symposium)*, The Welding Institute, Cambridge, England, June 11-13, 1973 (TTCP document).

Tooth, A.S. and Motashar, F.A. (1989). Radial loading of a cylindrical vessel through a rectangular rigid attachment. *International Journal of Pressure Vessels and Piping*, **37**, 345-363.

Timoshenko, S.P. and Woinowsky-Krieger, S. (1959). *Theory of plates and shells*, 2nd ed. New York: McGraw-Hill.

Uddin, Md. W. (1987). Large deformation analysis of plate-end pressure vessels. *International Journal of Pressure Vessels and Piping*, **29**, 46-65.

Viterbo, F. (1930). Sul problema della robustezza di cilindri cavi rinfortzati transversalmente sotto-posti da ogni parte a pressione esterna. *L'Ingegnere IV*, 446-456, 531-540 (also Bu-Ships Translation 354, 1949).

von Mises, R. (1929). Der kritische aussendruck zylindrischer rohre. *Stodola Festschrift*, Zurich, pp. 418-430.

von Sanden, K. and Gunther, K. (1920). Uber das festigkeitsproblem quersteifter hohlzylinder unter allseitig gleichmässigem aussendrück. *Weerft und Reederei*, **1** (8, 9, 10). (Also DTMB Translation 38, 1952).

von Sanden, K. and Gunther, K. (1921). *Weerft und Reederei*, **2** (17).

Watts, G.W. and Lang, H.A. (1952). The stresses in a pressure vessel with a flat head closure. *Transactions of the ASME*, **74**, 1083-1091.

Wenk, E. (1961). Pressure vessel analysis of submarine hulls. *Welding Journal*, **40** (6), 272s-288s.

Wilson, L.B. (1956a). *The deformation under uniform pressure of a circular cylindrical shell supported by equally spaced circular ring frames. Part 1 - Asymptotic method* (Report NCRE-R 337A). Dunfermline, Fife: Naval Construction Research Establishment.

Wilson, L.B. (1956b). *Part 2 - Fourier series method* (Report NCRL-R 337B). Dunfermline, Fife: Naval Construction Research Establishment.

Wilson, L.B. (1956c). *Part 3 - General discussion* (Report NCRE-R 337C). Dunfermline, Fife: Naval Construction Research Establishment.

Young, W.G. (1989). *Roark's formulas for stress and strain,* 6th ed. New York: McGraw-Hill.

# *Appendix 1*

## *Von Sanden and Gunther (Ignoring End Pressure)*

Differential Equation:

$$EI\,(d^4w/dz^4) + Ehw / R^2 = -p$$

Boundary Conditions:

$$\left.\begin{aligned} w(-z) &= w(z) \\ dw/dz &= 0 \\ 2EI\,(d^3w/dz^3) - pb &= Kw \end{aligned}\right\} \quad \text{at } z = L/2$$

Particular Solution of DE: $w = -pR^2 / Eh$

General Solution of DE:

$$w = A\sinh(\alpha z)\sin(\alpha z) + B\sinh(\alpha z)\cos(\alpha z) + C\cosh(\alpha z)\sin(\alpha z) + D\cosh(\alpha z)\cos(\alpha z) - pR^2 / Eh$$

Solution of Boundary Value Problem:

$$w = -(pR^2/Eh)\,[1 + 2\alpha(KR^2 - bEh)(A_-\sinh(\alpha z)\sin(\alpha z) - A_+\cosh(\alpha z)\cos(\alpha z))]$$

$$d^2w/dz^2 = -(pR^2)/Eh)\,[4\alpha^3(KR^2 - bEh)(A_+\sinh(\alpha z)\sin(\alpha z) + A_-\cosh(\alpha z)\cos(\alpha z))]$$

$$A_+ = [\sinh(\alpha L/2)\cos(\alpha L/2) + \cosh(\alpha L/2)\sin(\alpha L/2)] / H$$

$$A_- = [\sinh(\alpha L/2)\cos(\alpha L/2) - \cosh(\alpha L/2)\sin(\alpha L/2)] / H$$

$$H = R^2K\alpha\,[\sinh(\alpha L) + \sin(\alpha L)] + 2Eh\,[\cosh(\alpha L) - \cos(\alpha L)]$$

Frame Rigidity Constant:

$$K = E(A_f + bh) / R^2$$

Stresses:

$$\left.\begin{aligned} \sigma_z^m &= 0 \\ \sigma_\theta^m &= E\epsilon_\theta^m = Ew/R \end{aligned}\right\} \text{membrane}$$

$$\left.\begin{aligned} \sigma_z^b &= -[E\rho / (1 - \nu^2)] (d^2w/dz^2) \\ \sigma_\theta^b &= \nu\sigma_z^b \end{aligned}\right\} \text{bending}$$

($\rho$ ranges from -h/2 at the inner surface to +h/2 at the outer surface)

# *Appendix 2*

## *Von Sanden and Gunther (Including End Pressure)*

DE: $EI\,(d^4w/dz^4) + Ehw/R^2 = -\,p(1 - \nu/2)$

BCs:
$$\left.\begin{aligned} &w(-z) = w(z) \\ &dw/dz = 0 \\ &2EI\,(d^3w/dz^3) - pb = Kw \end{aligned}\right\} \quad \text{at } z = L/2$$

Particular Solution of DE: $w = -\,pR^2\,(1 - \nu/2) / Eh$

General Solution of DE:

$$w = A\sinh(\alpha z)\sin(\alpha z) + B\sinh(\alpha z)\cos(\alpha z) + C\cosh(\alpha z)\sin(\alpha z) + D\cosh(\alpha z)\cos(\alpha z) - pR^2/(1 - \nu/2)$$

Solution of BVP:

$$w = -\,(pR^2/Eh)\,[(1 - \nu/2) + 2\alpha(KR^2 - bEh)(A_-\sinh(\alpha z)\sin(\alpha z) - A_+\cosh(\alpha z)\cos(\alpha z))]$$

$$d^2w/dz^2 = -\,(pR^2/Eh)[4\alpha^3\,(KR^2 - bEh)(A_+\sinh(\alpha z)\sin(\alpha z) + A_-\cosh(\alpha z)\cos(\alpha z))]$$

Stresses:

$$\left.\begin{aligned} \sigma_z^{\,m} &= -\,pR/2h \\ \sigma_\theta^{\,m} &= Ew/R + \nu\sigma_z^{\,m} \end{aligned}\right\} \quad \text{membrane}$$

$$\left.\begin{aligned} \sigma_z^{\,b} &= -\,[E\rho/(1 - \nu^2)]\,(d^2w/dz^2) \\ \sigma_\theta^{\,b} &= \nu\sigma_z^{\,b} \end{aligned}\right\} \quad \text{bending}$$

# *Appendix 3*

## *Viterbo*

DE: $EI\,(d^4w/dz^4) + Ehw/R^2 = -\,p(1 - \nu/2)$

BCs:
$$\left.\begin{aligned} &w(-z) = w(z) \\ &dw/dz = 0 \\ &2EI\,(d^3w/dz^3) - pb\,(1 - \nu/2) = Kw \end{aligned}\right\} \quad \text{at } z = L/2$$

Particular Solution of DE: $w = -\,pR^2\,(1 - \nu/2) / Eh$

General Solution of DE:

As for Von Sanden and Gunther (Including end pressure)

Solution of BVP:

$$w = -\,[pR^2\,(1 - \nu/2)/Eh][1 + 2\omega_1(KR^2 - bEh)(A_- \sinh(\alpha z) \sin(\alpha z) - A_+ \cosh(\alpha z) \cos(\alpha z))]$$

$$d^2w/dz^2 = -\,[pR^2(1 - \nu/2)/Eh][4\alpha^3\,(KR^2 - bEh)(A_+ \sinh(\alpha z) \sin(\alpha z) + A_- \cosh(\alpha z) \cos(\alpha z))]$$

Frame Rigidity Constant: $K = E\,(A_f + bh) / R^2$

Stresses:

$$\sigma_z^{\,m} = -\,pR / 2h$$

$$\sigma_\theta^{\,m} = Ew / R + \nu\sigma_z^{\,m}$$

$$\sigma_z^{\,b} = -\,[E\rho / (1 - \nu^2)]\,(d^2w/dz^2)$$

$$\sigma_\theta^{\,b} = \nu\sigma_z^{\,b}$$

# *Appendix 4*

## *Salerno and Pulos*

DE: $EI\,(d^4w/dz^4) + (pR/2)\,(d^2w/dz^2) + Ehw/R^2 = -\,p(1 - \nu/2)$

BGs:
$$\left.\begin{aligned} &w(-z) = w(z) \\ &dw/dz = 0 \\ &2EI\,(d^3w/dz^3) - pb(1 - \nu/2) = Kw \end{aligned}\right\} \quad \text{at } z = L/2$$

Particular Solution of DE: $w = -\,pR^2\,(1 - \nu/2) / Eh$

General Solution of DE:

$$w = a\exp(\lambda_1 z) + b\exp(\lambda_2 z) + c\exp(\lambda_3 z) + d\exp(\lambda_4 z) - pR^2(1 - \nu/2) / Eh$$

with $\lambda_i$ the roots of

$$\lambda^4 + (pR/2EI)\,\lambda^2 + (hw/R^2I) = 0$$

giving $$\lambda_i = \pm\,\{2\alpha^2\,[-\,p/p^* \pm \sqrt{(p/p^*)^2 - 1}\,]\}^{1/2}$$

where $$p^* = 2hE/R^3\alpha^2 = 2h^2E/R^2\,\sqrt{3(1 - \nu^2)}$$

= critical pressure for axisymmetric elastic buckling of an unstiffened cylinder under uniform **axial** pressure.

As $\lambda_1 = -\,\lambda_2 = \{2\alpha^2\,[-\,p/p^* + \sqrt{(p/p^*)^2 - 1}]\}^{1/2}$

and $\lambda_3 = -\,\lambda_4 = \{2\alpha^2\,[-\,p/p^* - \sqrt{(p/p^*)^2 - 1}]\}^{1/2}$

the general solution reduces to:

$$w = A\sinh(\lambda_1 z) + B\cosh(\lambda_1 z) + C\sinh(\lambda_3 z) + D\cosh(\lambda_3 z) - pR^2\,(1 - \nu/2) / Eh$$

$$d^2w/dz^2 = A\lambda_1^{\,2}\sinh(\lambda_1 z) + B\lambda_1^{\,2}\cosh(\lambda_1 z) + C\lambda_3^{\,2}\sinh(\lambda_3 z) + D\lambda_3^{\,2}\cosh(\lambda_3 z)$$

Solution of BVP:

$$A = C = 0$$

$$D = - B [\lambda_1 \sinh (\lambda_1 L/2)] / [\lambda_3 \sinh (\lambda_3 L/2)]$$

$$B = \frac{p(1 - \nu/2) (KR^2 - bEh) \lambda_3 \sinh (\lambda_3 L/2)}{Eh [G_1 \lambda_- \sinh (\lambda_3 L/2) - G_3 \lambda_1 \sinh (\lambda_1 L/2)]}$$

where $G_i = 2EI \lambda_i^3 \sinh (\lambda_i L/2) - K \cosh (\lambda_i L/2)$

Stresses:

$$\sigma_z^m = - pR / 2h$$

$$\sigma_\theta^m = Ew / R + \nu \sigma_z^m$$

$$\sigma_z^b = - [E\rho / (1 - \nu^2)] d^2w/dz^2$$

$$\sigma_\theta^b = \nu \sigma_z^b$$

# *Appendix 5*

## *Wilson's Asymptotic Method*

DE: $EI\,(d^4w/dz^4) + (pR/2)\,(d^2w/dz^2) + Ehw / R^2 = -\,p(1 - \nu/2)$

BCs:

$$\left.\begin{aligned} &w(-z) = w(z) \\ &dw/dz = 0 \\ &2EI\ (d^3w/dz^3) - pb(1 - \nu/2) = Kw \end{aligned}\right\} \quad \text{at } z = L/2$$

Assumed Form of Solution:

$$w = pw_1 + p^2w_2$$

Resulting Pair of BVPs for $w_1$ and $w_2$:

$$EI\,(d^4w_1/dz^4) + Ehw_1 / R^2 = -\,(1 - \nu/2)$$

$$\left.\begin{aligned} &w_1(-z) = w_1(z) \\ &dw_1/dz = 0 \\ &2EI\,(d^3w_1/dz^3) - b(1 - \nu/2) = Kw_1 \end{aligned}\right\} \quad \text{at } z = L/2$$

$$EI\,(d^4w_2/dz^4) + Ehw_2 / R^2 = -\,(R/2)\,(d^2w_1/dz^2)$$

$$\left.\begin{aligned} &w_2(-z) = w_2(z) \\ &dw_2/dz = 0 \\ &2EI\,(d^3w_2/dz^3) = Kw_2 \end{aligned}\right\} \quad \text{at } z = L/2$$

Solutions of BVPs:

$w = pw_1$ is the linear, Viterbo solution.

$$w_2 = C_1 \sinh(\alpha z) \sin(\alpha z) + C_2 \cosh(\alpha z) \cos(\alpha z) + C_3 z \sinh(\alpha z) \cos(\alpha z) + C_4 z \cosh(\alpha z) \sin(\alpha z)$$

$C_1$, $C_2$, $C_3$ and $C_4$ are determined from the boundary conditions. Fairly complicated expressions result, as shown by Wilson (1956a).

Frame Rigidity Constant (K): As for Wilson's Fourier Series Method.

Stresses: As for Wilson's Fourier Series Method.

# *Appendix 6*

## *Wilson's Fourier Series Method*

DE: $EI\,(d^4w/dz^4) + (\nu EI/R^2 + pR/2)\,d^2w/dz^2 + Ehw/R^2 = -\,p(1 - \nu/2)$

BCs:

$$\left.\begin{aligned} &w(-z) = w(z) \\ &dw/dz = 0 \\ &2EI\ (d^3w/dz^3) - pb(1 - \nu/2) = Kw \end{aligned}\right\} \quad \text{at } z = L/2$$

Assumed Form of Solution:

$$w(z) = \bar{w}(o) + (2/\pi) \sum_{n=1}^{\infty} \bar{w}(n) \cos(2\pi nz/L)$$

$$\bar{w}(n) = \int_0^{\pi} w(2\pi z/L) \cos(2\pi nz/L)\, dz$$

$$= \text{Fourier coefficients}$$

Solution of BVP: See Wilson (1956b).

Stresses:

$$\left.\begin{aligned} \sigma_z^{\,m} &= -\,pR/2h \\ \sigma_\theta^{\,m} &= Ew/R + \nu\sigma_z^{\,m} \end{aligned}\right\} \quad \text{membrane}$$

$$\left.\begin{aligned} \sigma_z^{\,b} &= -\,E\rho\,[\nu w/R^2 + (d^2w/dz^2)]/(1 - \nu^2) \\ \sigma_\theta^{\,b} &= -\,E\rho\,[w/R^2 + \nu\,(d^2w/dz^2)]/(1 - \nu^2) \end{aligned}\right\} \quad \text{bending}$$

($\rho$ ranges from -h/2 at the inner surface to +h/2 at the outer surface of the shell).

Frame Rigidity Constant:

$$K = E(A_f/R_f^{\,2} + bh/R^2) + 3E(I_f/R_f^{\,4} + bh^3/12R^4) \doteqdot E(A_f/R_f^{\,2} + bh/R^2)$$

# *Appendix 7*

## *Stress Concentration due to Bulkhead or Heavy Frame*

Calculation of the hull plating deflection using equation (55) in Section 5.6.3 requires knowledge of the rigidity constant $K_H$ for the heavy frame. The special cases $K_H = K$ (the normal ring stiffener rigidity constant) and $K_H = \infty$ (perfectly rigid bulkhead) have been discussed in Section 5.6.3. Expressions presented here allow $K_H$ to be calculated for intermediate cases. The deflection can then be calculated using equation (55) and the stresses using expressions in Appendix 6.

The assumption is made that the additional deflection due to the heavy frame is the same for a uniformly framed cylinder as for an infinite cylindrical shell. This is a reasonable assumption for typical submarine hull deflections and frame spacings.

For the case of frames only moderately more rigid than the normal frames, Wilson's (1956c) expressions for K in Appendix 6 may be used.

Wilson (1956c) also gives an expression for deep frames (depth > 0.2 × shell radius):

$$K_H = Eb\,(t_f + h) / R^2 + ER_1^2 / R\,[(1 + \nu)\beta - (1 - \nu)\gamma R_1^2]$$

where $t_f$ and additional parameters are defined in Figure A7-1 and:

$$\beta = \mp R_1^2 R_2^2\,[Eh_w \pm (1 - \nu)\,R_2\lambda_f] / S$$

$$\gamma = \pm R_1^2\,[Eh_w \mp (1 + \nu)\,R_2\lambda_f] / S$$

$$\lambda_f = Eh_f f / a^2$$

$$S = h_w R_1^2\,[Eh_w \mp (1 + \nu)\,R_2\lambda_f] - h_w R_2^2\,[Eh_w \pm (1 - \nu)\,R_2\lambda_f]$$

The upper and lower signs refer to external and internal frames respectively.

For a bulkhead idealized as a flat circular plate of thickness t and radius R, Sokolnikoff (1956) shows that the radial deflection and stresses due to uniform radial pressure p on the circumference are:

$$w_r = -\,p\,(1 + \nu)(1 - 2\nu)\,r / E$$

$$\sigma_r = \sigma_\theta = -\,p$$

Therefore the rigidity constant is:

$$K_H = tE / R(1 + \nu)(1 - 2\nu)$$

For the case t = 25 mm, E = 205 GPa, R = 5 m and ν = 0.3, the value of $K_{II}$ is 2 GPa and the deflection of the circumference is $w_r$ = 0.04 mm for a pressure of 3 MPa. The bulkhead is almost perfectly rigid (the rigidity constant for a typical ring stiffener is of the order of 10% of this value).

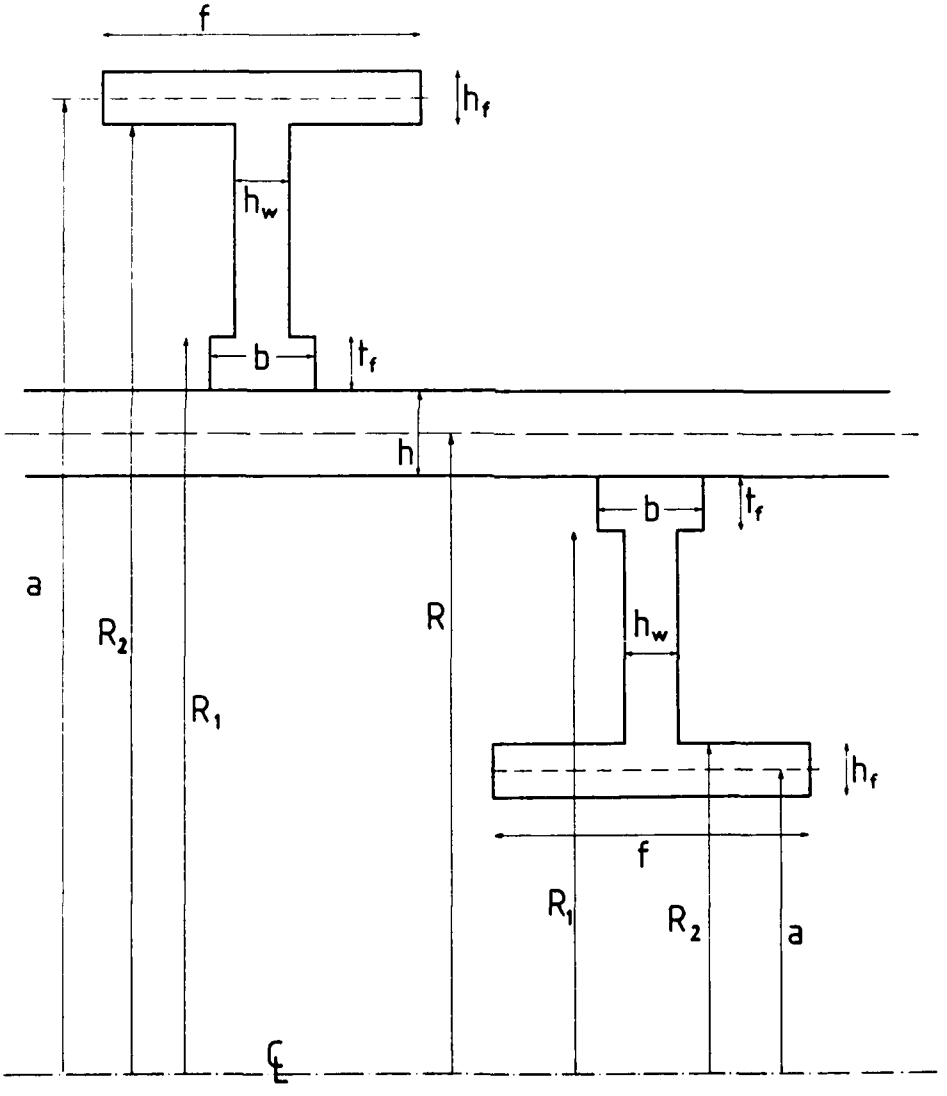


*Figure A7-1 : Notation used for the calculation of the frame rigidity constant. Both external and internal frames are considered.*

SECURITY CLASSIFICATION OF THIS PAGE **UNCLASSIFIED**

DOCUMENT CONTROL DATA SHEET

| REPORT NO. | AR NO. | REPORT SECURITY CLASSIFICATION |
|---|---|---|
| MRL-TR-90-26 | AR-006-326 | Unclassified |

TITLE

Analytical Calculations of Fatigue Loading of Submarine Hulls


AUTHOR(S)

I.M. Robertson

CORPORATE AUTHOR

DSTO Materials Research Laboratory
PO Box 50
Ascot Vale Victoria 3032



| REPORT DATE | TASK NO. | SPONSOR |
|---|---|---|
| November, 1990 | NAV 88/152 | DNA |

| FILE NO. | REFERENCES | PAGES |
|---|---|---|
| G6/4/8-3901 | 73 | 76 |

CLASSIFICATION/LIMITATION REVIEW DATE

CLASSIFICATION/RELEASE AUTHORITY
Chief, Materials Division

SECONDARY DISTRIBUTION

Approved for public release

ANNOUNCEMENT

Announcement of this report is unlimited

KEYWORDS

Stress
Stress Concentration
Weld
Ring Stiffened Cylinder

SUBJECT GROUPS



ABSTRACT

Fatigue is a potential failure mode of submarine pressure hulls. Australia's new Type 471 submarines will be constructed from a new high strength steel. The higher design loadings made possible by the higher strength make fatigue an even more significant consideration than in other designs. The stress analysis of submarine pressure hulls under hydrostatic loading is reviewed. The main emphasis is on analytical methods of calculation as opposed to numerical (e.g. finite element) methods, and on the calculation of the fatigue loading rather than the calculation of buckling pressure. Because of the emphasis on fatigue, stress concentrations, residual stresses and the interaction between residual and applied stresses are considered.